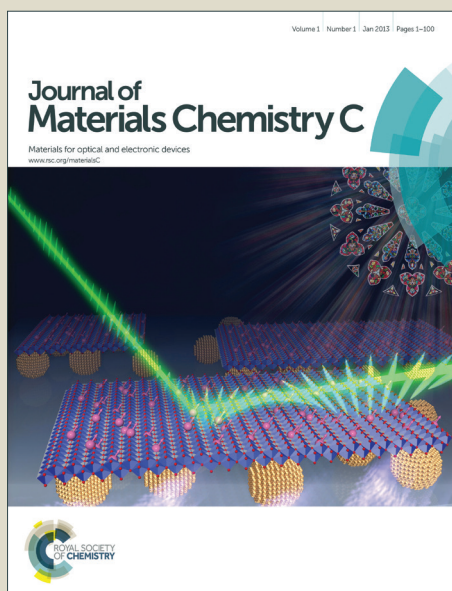


Journal of Materials Chemistry C

Accepted Manuscript



This article can be cited before page numbers have been issued, to do this please use: Y. Aleeva and B. Pignataro, *J. Mater. Chem. C*, 2014, DOI: 10.1039/C4TC00618F.



This is an *Accepted Manuscript*, which has been through the Royal Society of Chemistry peer review process and has been accepted for publication.

Accepted Manuscripts are published online shortly after acceptance, before technical editing, formatting and proof reading. Using this free service, authors can make their results available to the community, in citable form, before we publish the edited article. We will replace this *Accepted Manuscript* with the edited and formatted *Advance Article* as soon as it is available.

You can find more information about *Accepted Manuscripts* in the [Information for Authors](#).

Please note that technical editing may introduce minor changes to the text and/or graphics, which may alter content. The journal's standard [Terms & Conditions](#) and the [Ethical guidelines](#) still apply. In no event shall the Royal Society of Chemistry be held responsible for any errors or omissions in this *Accepted Manuscript* or any consequences arising from the use of any information it contains.

ARTICLE

Recent advances in upscalable wet methods and ink formulation for printed electronics

Cite this: DOI: 10.1039/x0xx00000x

Y. Aleeva^a and B. Pignataro^{a,*}Received 00th January 2012,
Accepted 00th January 2012

DOI: 10.1039/x0xx00000x

www.rsc.org/

This review deals with the use of solution processing approaches for organic electronics with a focus on the material ink formulations as well as on their applicability. The solution processing techniques include methods like gravure printing, screen printing and ink-jet printing. Basic principles of each approach are understood and fundamental correlations between material (metals, semiconductors, dielectrics) ink properties and final device performances can be drawn. Nevertheless, solution processing methods have the potential to evolve among the most promising tools in organic device fabrication techniques and have already been applied successfully in the fields of organic thin film transistors, solar cells and biosensing devices.

Introduction

Electronics has experienced an enormous breakthrough during the past decade leading to the development of efficient, scalable, and rational processing techniques allowing the production of smaller, better and faster electronic devices for application in everyday life. However, the wide use of traditional silicon technology for almost all electronic device fabrication represents practical limitation to flexibility and low cost. In addition, the complexity, the difficulty in patterning large areas, and the limited range of materials that can be directly patterned all represent significant disadvantages. In this respect, solution processable materials represent a good alternative for traditional inorganic materials due to their numerous advantages. Solution processable materials benefit from ease of device fabrication, improvement in functionality, large area applications, compatibility with light weight and mechanically flexible base materials, as well as good control of their electrical, optical and magnetic properties [1-3]. Moreover, printable electronics allows the improvement of material performance by printing, due to the possibility to reduce defects in printed structures, the possibility to fabricate new and complex architectures and the possibility to transform materials or thin deposits which are usually unusable for applications to functional structures [4-6].

What above led to the evolution of the interdisciplinary field of printed electronics (PE). PE has emerged as a field of electronics, in which electronically active components (semiconducting layer, electrodes, dielectrics etc.) are built in a large fashion by molecular materials [7,8]. In this context, solution processing, low cost, low energy and conducting polymers are typical keywords associated with polymer electronics. One of the most important advantages of conducting polymers is the variety of device fabrication methods that may be used to form them into useful devices.

To realize PE, one of the key issues is how to fabricate the ordered structures in a planned manner since various properties of

organic molecules and molecular materials are of anisotropic nature, and consequently the functions of molecular assemblies depend strongly on the way molecules are organized in the device [6]. It is accepted that the ultimate goal for solution-processed electronics is the development of a fabrication process that does not waste materials by depositing each layer at the same time that patterning is done. High performance, stability, and low temperature processing temperatures are also required. To achieve these goals, it is needed to fabricate the semiconductor and dielectric components of electronic devices via high throughput, low-temperature solution processing methods such as spin-coating, casting, or printing [10-15].

However, for printed electronics, in order to succeed as an efficient and economic technology, more effort must be directed towards large area fabrication combined with high throughput processing such as coating, printing and layer-by-layer deposition methods. Such processing techniques are associated with low-cost and low energy consumption, large-scaling and large-area fabrication, therefore favouring the advancement of various wet processing techniques. The driving force for research within the field lately revealed the potential of the technology to enable knowledge transfer and scaling up from laboratory into industrial sectors. That is why it is important to design new techniques to accelerate their practical application. Moreover, the device materials ought to be formulated into solvent-based inks, which are then deposited by printing processes including ink-jet, gravure, screen printing etc..

In this respect, semiconductors, conductors and dielectrics solution-processability is the key prerequisite for low-cost device fabrication [11]. In addition to the substrate surface properties, the most crucial part in printing technology affecting both printing conditions and pattern resolution is the ink and its physical properties like viscosity and surface tension. Moreover, different printing techniques require substantially different ink rheological properties. For example, ink-jet printing requires the use of dilute ink solutions while more viscous inks are typically used in gravure

printing [16]. Furthermore, in ink-jet printing the ink chemistry and formulations define the drop ejection characteristics and the compatibility with the print head system, as well as the quality of the printed films [17]. The ideal ink for conductive features containing conductive materials would be low cost, easy to prepare, store and jet, and would yield high conductivity values after deposition and post-processing [18].

Printed electronics applications of conventional and digital printing require well-defined and uniform deposits without solute segregation. Moreover, the performance and life-time of electronic devices critically depends on the uniformity of the patterns. The resolution of micrometre-size patterns of most direct-printing techniques is limited to typically 20–50 μm . Such difficulties are associated with poor control of flow and spread of liquid inks on surfaces [19].

In terms of ink formulation, the choice of solvent is extremely important and currently pushing towards the use of water as it is non-toxic, cheapest and an environmentally friendly solvent. However, the development of suitable water-based inks for printing on plastic substrates has met certain challenges. The substrate can be quite difficult to print upon using conventional water-based inks, the major problems including pinhole formation and lack of adhesion of the ink to the substrate. This is related to the fact that the surface energy of typical plastic substrates are much lower than that of water, resulting in poor wetting of these materials by water-based inks. This problem has been partly overcome in the art by inclusion in the ink composition of at least one organic co-solvent which reduces the ink's surface tension [20].

Herein, we aimed to guide the reader through the current state of art and challenges in the context of pattern formation and various PE devices fabrication. At first, we introduce the fundamental principles of the main printing techniques. Then we discuss the key points related to inks formulation along with their interaction with the substrate that is crucial for various electronics applications such as organic diodes, organic circuits, thin film transistors, photovoltaic cells etc. In this respect, the application requirements determine the range of device and materials specifications such as critical dimensions, electronic responses and intrinsic materials and interface parameters.

2. Printing techniques

In order to address advantages and disadvantages of solution processing techniques for organic electronics and to gain an overview of the challenges and possibilities of each technique described we would consider only mass printing techniques allowing high processing speeds and up-scaling towards roll-to-roll production. We can differentiate conventional and digital printing techniques for polymer electronics. Conventional mass-printing techniques represented in here include gravure and screen printing, while the use of ink-jet printing is discussed as an example of digital printing method. In this section an introduction to printing technologies and the available instrumentation is given.

2.1. Gravure printing

Gravure printing is an abundant and cost-effective patterning process employed in everyday life for high volume prints such as newspapers, magazines, catalogues and packaging. The use of the gravure printing for applications in electronics dates back to 1980's [21]. Nowadays, gravure printing application for the preparation of solar cells, organic light emitting diodes and polymer field effect transistors (FET) is reported [22–24].

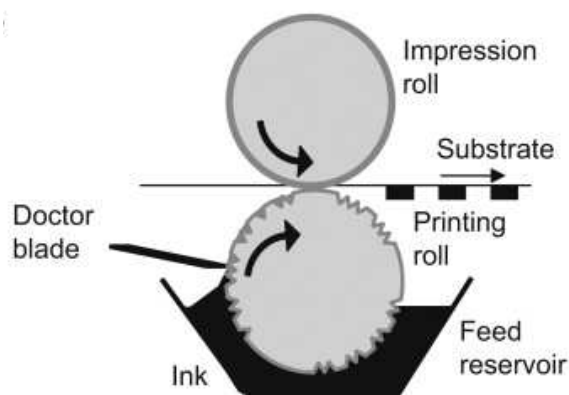


Fig. 1 Schematic illustration of gravure printing method (Reprinted from *Solar Energy Materials and Solar Cells*, 94/10, P. Kopola, T. Aernouts, S. Guillerez, H. Jin, M. Tuomikoski, A. Maaninen, J. Hast, High efficient plastic solar cells fabricated with a high-throughput gravure printing method, Pages No.1673-1680, Copyright (2010), with permission from Elsevier [23])

In the gravure printing process, represented in Fig. 1 (a), the ink is continuously fed from the ink bath and doctored in the engraved cells on the gravure cylinder. Typical cell densities are between 220 and 400 cells per inch, with a cell depth $\sim 40 \mu\text{m}$ and width $< 100 \mu\text{m}$ [25]. Consequently, a rubber roller or pad picks up the ink from the gravure cells by rotating over the gravure or by pressing on it. Then the roller or the pad with the ink on it is brought into contact with the substrate to transfer the ink through a similar movement [26].

Roller type printing offers cost effective, high volume manufacturing of flexible electronic devices and pad printing, in turn, allows patterning on non-planar surfaces and increased time of resolution [26]. In addition, gravure printing maintains features desirable in large scale manufacturing such as very high speed, of up to 1 m/s and resolution from tens of μm to several nanometers [27, 28]. It can either be used as a sheet-to-sheet or a roll-to-roll process.

Scale-up of printability of photoactive and hole transport layers in electronic devices by gravure printing is highly dependent on engraving parameters of the cylinder, ink properties and printing parameters. Noteworthy, the shape and thickness of the final imprint is greatly affected by the pattern and depth of the engraved cells in the gravure cylinder. Therefore, engraving parameters such as cell density, depth, width, screen angle and stylus angle can be adjusted in order to optimise the cylinder design for the printing ink and vice versa [23]. Moreover, careful optimization of the ink's surface tension is important, as the quality of the print is highly dependent on ink rheology, web speed, and the pressure of the impression cylinder [29].

Gravure inks need to be sufficiently fluidic to fill the cells of the gravure cylinder. Therefore, the inks must have sufficiently low shear viscosities (in the range of 0.05–0.2 Pa·s) and a sufficiently low surface tension, thus inks usually are water or solvent based [10].

In the case of thin film transistor (TFT) fabrication, smooth and uniform semiconductor film morphology is needed for a pinhole-free gate dielectric film deposition. When low viscosity inks are employed for gravure printing, it results in the formation of homogeneous films, which are often required for organic electronics [16, 30]. For instance, Yan et al. reported on gravure printed n-type polymer TFT on polyethylene terephthalate (PET) substrates exhibiting large gains ($> 25\text{--}60$) and operating in ambient

conditions. They scrutinised the effect of the semiconductor ink formulation viscosity and gravure cylinder cell volume suggesting that decrease in gravure cell depth/volume ratio resulted in formation of smooth fibre-like morphology comparable to conventional Si-SiO₂ substrates [16].

In addition, the printability of the ink should be controllable, i.e. the ink should not spread across the engraved pattern, as this feature is needed when processing solar cell modules, which require patterning of the printed layers [23].

In summary, gravure printing is attractive for printing polymer electronic devices due to its high throughput, wide choice of substrates and inks, ability to control inks, cylinder and substrate temperature. The ability to print blend films of n- and p-type organic semiconductors and light-emitting polymers shows that gravure printing can be used to manufacture all the essential elements of organic electronics [28].

2.2. Screen printing

Screen printing, as a technique for creating a two-dimensional pattern, started in the beginning of the 20th century and has been touted as the most versatile of all printing techniques [30]. The operating principle of screen printing is represented in Fig. 2 (a). The squeegee moves against the screen and presses the ink paste through. The screen represents the mesh, normally made of porous fabric or stainless steel. The desired motif, i.e. the stencil, can be photochemically or manually defined in the mesh [31]. The viscosity of the ink, its wetting of the substrate, and other parameters determine the functionality of this method. In particular, mesh dimensions itself (such as thickness of 30-385 μm for polyester and 40-215 μm for stainless steel wires with meshings of 30-200 threads/cm) can limit the resolution of the printed patterns [32].

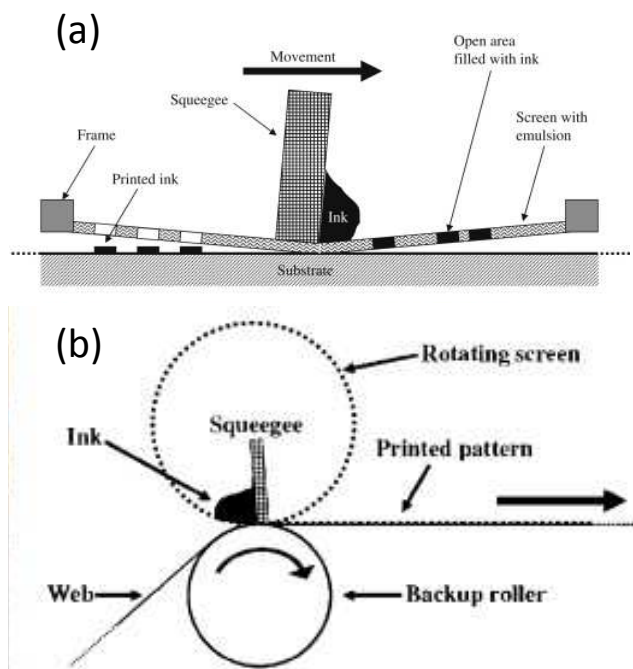


Fig. 2 Schematic illustration of (a) the screen-printing process (b) a rotary screen printer (Reprinted from *Solar Energy Materials and Solar Cells*, 93/4, F.C. Krebs, Fabrication and processing of polymer solar cells: A review of printing and coating techniques, Pages No.394-412, Copyright (2009), with permission from Elsevier [30])

There are two types of screen printing, namely flat-bed screen printing and rotary screen printing with the significant differences in the operation of the two techniques. The advantages of flat-bed screen printing include low-cost of the mask, large-area printing (up to 10 m²), and possibility of making one print at a time and ease of readjusting between each print if needed. In rotary screen printing (Fig. 2 (b)), however, the ink is contained inside the rotating cylinder with a fixed internal squeegee and the ink is less exposed to the surroundings. In this technique the mask is a lot more expensive, however, this method is a true roll-to-roll printing technique in terms of speed, edge definition/resolution, and achievable wet thickness [29]. Screen printing is mainly used for the printing solar cells, fuel cells, organic field effect transistors (OFET), organic thin film transistors (OTFT), but also screen printing of active layers have been reported [33-37].

Screen printing inks are generally characterized as liquid inks with shear thinning characteristics. The viscosity of a screen printing ink can vary between 0.05 and 5 Pa·s. Ideal viscosity behavior is a high rest viscosity, a low viscosity at high shear, and a fast viscosity recovery time. To achieve a smooth surface when printing on a solid surface requires a long recovery time, thereby allowing the ink to flow after printing to achieve a uniform coating. The flow of ink through the screen can cause defects during the printing of lines or solid areas. Ink has to flow around the individual threads of the screen mesh. If the ink flow is insufficient, local starvation of ink occurs which results in a phenomenon called mesh marking (a regular patterning of the surface or line width). The amount of mesh marking is a function of the printing conditions and the ink characteristics [10].

Screen printing benefits from its simplicity, compatibility with variety of organic inks and ability to print under ambient pressure. All this enables low-cost printing on flexible substrates with good reproducibility [38]. Moreover, in contrast with gravure printing, screen printing is a technique that inherently allows for the formation of a thicker wet layer (10-500 μm) and thereby also a very thick dry films, which can be useful for printed electrodes where high conductivity is needed [29]. The downside of this method when employed for producing large feature sizes shows a relatively low resolution (>75 μm) [38]. This is especially problematic for the active layers where good control of the film thickness and morphology is required. Another complication is the exposure of the ink to the atmosphere during printing. The critical requirement in this respect is that the ink must not dry out on the mask and an open time of several hours is required for an industrial process. If volatile solvents are used they dry up in the screen printing mask and thus deteriorate the definition of the printed pattern [30].

2.3. Ink-jet printing

Ink-jet printing (Fig.3) is considered to be one of the key technologies for various industrial processes. The advantages of ink-jet printing include accurate and rapid deposition of a broad range of functional materials (ink compositions) in a large area at low cost, and a possibility to deposit very small amounts of the material [39,40]. Moreover, the ink-jet printing is a non-contact and maskless method and, therefore, the contamination of substrate is minimized. Ink-jet printing can be used in an automated fabrication allowing selective patterning of the surface [32,41].

Ink-jet printer can operate in one of the two modes, namely continuous mode and drop-on-demand (DOD) mode. In the continuous mode, the ink is ejected through a nozzle to form a liquid jet. Here, surface tension driven break-up splits the jet into uniformly spaced and sized droplets by a periodic perturbation. Continuous mode ink-jet printing is mainly used for high speed graphical

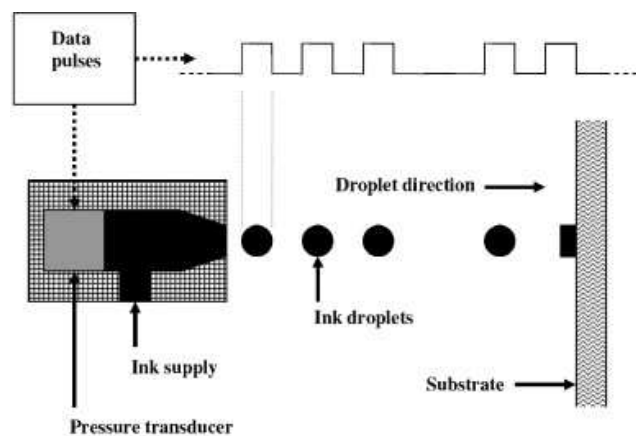


Fig. 3 Schematic illustration of an ink-jet printing process using a data pulse train to generate droplets on demand via a pressure transducer (Reprinted from *Solar Energy Materials and Solar Cells*, 93/4, F.C. Krebs, Fabrication and processing of polymer solar cells: A review of printing and coating techniques, Pages No.394-412, Copyright (2009), with permission from Elsevier [30])

applications such as textile printing and labeling. Drop-on-demand mode, in turn, is characterized by smaller drop size and higher placement accuracy. In this mode, ink droplets are pumped through a nozzle from a reservoir by acoustic pulse. The pulse can be generated either thermally or piezoelectrically [32].

In a thermal DOD ink-jet printer (or bubble-jet) ink is heated locally (heating temperature ~ 300 °C for aqueous inks) by electrical pulses applied to nozzle heaters. Generated joule heating is used to form a rapidly expanding vapor bubble that pumps an ink droplet through a nozzle. Polymer printing via thermal DOD can be quite limited as it normally uses water as solvent, although non-aqueous thermal inks are available [39].

Piezoelectric DOD ink-jet printing on the other hand, relies on the deformation of piezoelectric material such as lead zirconium titanate. Here, the pressure impulses are created by electrical pulses applied to the piezoelectric element. Generated impulses vary rapidly the volume of ink chamber, thus propelling the droplets. Such set-up allows to prevent the heating associated with thermal printheads, and provides good control over the shape of pressure pulse (i.e. rise and fall time) [32]. Furthermore, a wide variety of solvents can be used for piezoelectric DOD [39].

To note, the resolution of the ink-jet process is determined by such parameters as the nozzle diameter (\approx the droplet diameter) along with the statistical variation of the droplet flight and spreading on the substrate, and by the stability and accuracy of the jetting process. To overcome this problem hybrid ink-jet processes employing photolithography have been demonstrated allowing to increase the resolution from the average value of the feature size of 50–100 μm up to 1–30 μm [40, 44].

Ink-jet inks are generally described as having a narrow viscosity range 2–25 mPa·s which allows these inks to flow through the print head and be propelled using the printing mechanisms, while inks with viscosities of 40 mPa·s and above are not ink-jet printable at room temperature. Formulation is limited by the jetting process, therefore it should be taken into consideration that high volume percent loading with metal particles typically results in a viscosity outside the range printable by jetting. Moreover, the ink solvent should be compatible with the entire printhead mechanism [10].

In the past decades, the ink-jet printing of polymers has attracted a lot of attention due to the growing interest in the production of plastic electronic devices, due to their flexibility, low weight, ease of processability and low cost manufacturing [39, 41].

With the use of ink-jet printing techniques, the deposition of all parts of the transistor device, contact electrodes, semiconducting layers, and insulating materials is possible. In particular, ink-jet printing has enabled the production of full-color polymer light emitting diodes, organic electronic components and circuits using various polymer electronic materials [32,39,40,45].

Ink-jet printing can also be seen as a synthetic tool. Recently developed reactive ink-jet printing (RIP) technique allows forming a functional material by dispensing multiple reactants from separate nozzles onto a substrate [46]. The advantages of RIP include increased yield of reactions, reduced material consumption and possibility of patterning the products into required device geometry [47].

For example, Abulikemu et al. reported synthesis of self-assembled Au nanoparticles as small as (8 ± 2) nm by using RIP and a unique solvent/precursor system. The structures were fabricated *in-situ* by ink-jet printing a mixture of solvents containing a capping/reducing agent and a dispersion solvent, followed by successive printing of organic gold precursor. A printed substrate was then thermally cured at 120°C for 3 h. [48]

Reactive ink-jet printing has also been applied to create polymers *in situ* and on substrates. Krober et al suggested *in-situ* of cross-linked thermoset polyurethane materials with spatial resolution in the range of tens of microns. In this method, droplets of two inks, one containing isophorone diisocyanate and the other consisting of poly(propylene glycol), were printed from separate nozzles. Polyurethane structures were formed within minutes following the droplet merging on the substrates [49]. This approach could be developed further and adopted as a low-cost and reliable high-throughput method for the preparation of various types of structures on a variety of substrates.

3. Ink formulation

The diversity of materials that can be deposited by solution methods for PE device fabrication has expanded dramatically over the past decade. In the recent years, solution processable organic and hybrid materials, used for fabrication of electronic device components, including semiconductors, insulators and electrodes, have attracted the attention of the scientific community. With the rise of functional printing there is a need of understanding the printability of a greater range of materials. A particular effort is addressed to the optimization of various parameters such as the accurate selection of precursors, solvents, and additives, which need to be tailored to the deposition and processing techniques. In this section, we will review the current achievements on ink formulation used for solution processing of various components of printed electronic devices.

3.1. Semiconducting layers and electrode materials formulation

3.1.1. Polymer based inks

Semiconducting materials are crucial for the performances of OTFT, organic light emitting diodes (OLED), solar cells etc. Therefore, in the past decade intensive research was focused on the design and synthesis of new materials and different types of organic semiconductors (such as polymers, carbon nanotubes and graphene) for semiconductor layers fabrication via bottom up solution processing enabling flexible and low-cost manufacturing [50].

Since their discovery in 1977, conjugated polymers are interesting candidates for electronic devices due to their

semiconducting properties [51]. One of the major advantages of conjugated polymers is that the polymer can be tailored to optimize the final device properties, for example by attaching side chains to the polymer backbone for an improved solubility or electron affinity. The possibility of altering the material properties and the application of solution-based direct-printing techniques, such as coating or printing, to the deposition and direct-write patterning of functional materials classifies conjugated polymers as promising materials for smaller, flexible and low cost electronic devices. Furthermore, polymers offer significant advantages in terms of solution rheology and mechanical properties. Semiconducting polymers, however, currently are characterized by low electrical conductivity and poor electrical and thermal stabilities, hence, limiting their application [52]. Therefore, such parameters as their structure, molecular weight, concentration and solvent have to be taken into account to enable ink formulations with tuned rheological properties when using polymers [41, 53, 54].

Polythiophenes is one of the most important class of semiconducting polymers currently known [55]. As far as conductive polythiophenes are concerned, impressive progress has been made in developing materials with fluorene bithiophene (F8T2) [50], poly[3,4-bis(2,5,8-trioxanonyl)thiophene (PBTTT) [49], poly(3,3'-didodecylquaterthiophene) (PQT) [57], poly(3-hexylthiophene) (P3HT) [58], poly(ethylenedioxythiophene) (PEDOT) [59] being among the most investigated polymers.

For instance, poly(3,4-ethylenedioxythiophene):poly(styrenesulfonic acid) (PEDOT:PSS), an important derivative of polythiophene, is an attractive working electrode material associated with its high conductivity, low red-ox potential, good film-forming properties and long-term stability [60]. Accurate control over PEDOT:PSS ratio and/or film morphology allows tuning of the conductivity of PEDOT:PSS thin films [61-63]. Meixner et al. studied several commercially available PEDOT:PSS inks, including Baytron P as PEDOT:PSS in an aqueous dispersion, CPP 105 D as PEDOT:PSS with quick drying solvents (e.g. n-methyl-2-pyrrolidone (NMP), isopropyl alcohol), Baytron P in combination with 0.5 weight percent of the surfactant Tween 20 (BT), and Baytron P in the combination with 21 weight percent Tween 20 and 12 weight percent methanol (BTM) [63]. All inks studied exhibited non-newtonian behavior as shown in Fig. 4. With regards to printability, the intervals of the energy number En (ratio of kinetic and surface energy respectively, depends on rheological properties of the ink) and the inverse Ohnesorge-number Z^{-1} (depends on the printing system) for employed inks must be between zero to one and one to ten respectively, to avoid drop splashing on the substrate [64, 65]. The printability conditions were fulfilled for all the inks except the BTM sample, suggesting that the latter did not yield a stable printing process. Moreover, inks were also used to print source and drain electrodes of OFET via print-on-position method revealing that CPP 105 electrode resulted in scale structure due to fast drying behavior, while addition of Tween to Baytron P produced straight and homogeneous lines (Fig. 4 (b)). The drain currents were also measured (Fig. 4 (c)) and values differ by one order of magnitude as affected by the sheet resistance of the electrode material.

Kopola et al. studied PEDOT:PSS ink formulations for gravure printing of active layers in solar cell fabrication. They scrutinized suitable chemicals which, when combined with a PEDOT:PSS dispersion, lower the surface tension while maintaining a good printability and electro-optical performance. To do so, five different formulations of PEDOT:PSS inks based on commercially available Clevios P VP AI4083 (H.C. Starck, average solid content 1.5%) which also contained N-methylpyrrolidone (NMP), 2-propanol, isopropyl alcohol (IPA) as solvents, dimethylsulfoxide (DMSO) as conductivity enhancer, and such additives as Tween 80,

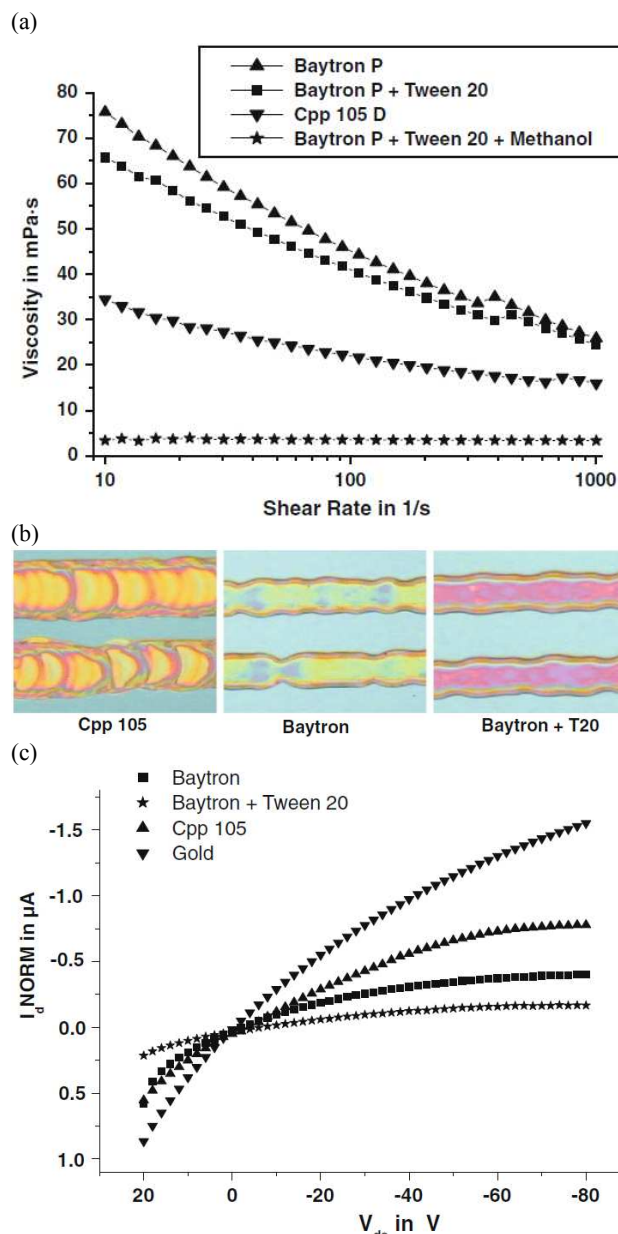


Fig. 4 a) Viscosity versus shear rate measured at 20 °C, b) Source and drain electrodes on a siliconoxide substrate, c) Comparison of normalized drain currents between gold and polymer inks (Reprinted from *Microsystem Technologies*, Vol. 14, R. M. Meixner, Characterization of polymer inks for drop-on-demand printing systems, Pages No.1137-1142, Copyright (2008), with permission from Springer [63]).

polyvinyl alcohol water solution were studied. Therefore, the effect of several chemicals on the surface tension, viscosity and printability and hole transport properties was investigated [23]. Addition of 25-50 wt% of IPA to PEDOT:PSS reportedly decreased the surface tension to 27-22 mN/m respectively and the printability improved significantly. Moreover, the addition of NMP allowed to slow down the drying process. Also, NMP serves as a lubricant between the doctor blade and the cylinder, diminishing the wear of the printing elements and facilitating the cleaning of the equipment. Furthermore, the effect of additives on film formation was studied suggesting that polyvinyl alcohol increased the surface tension since it dissolves in water. Note, the uniformity of the printed PEDOT:PSS film was

improved when 10–40 wt% polyvinyl alcohol was used in the formulation. However, it promoted ink accumulation along the edges of the engraved areas. Using Tween 80 as additive, on the other hand, improved the resolution by making the printed features more easily defined. Accurate tailoring of ink formulation allowed to produce solar cell devices with gravure printed PEDOT:PSS hole transport layers and poly-3-hexylthiophene (P3HT) / [6,6]-phenyl-C61-butyric acid methyl ester (PCBM) photoactive layers exhibiting power conversion efficiency of 2.8%.

In the last several years a rapid progress have been made in developing n-type conducting polymers including siloles, rylene diimides, n-type acene- and fullerene- based polymers, and several ink formulations are nowadays commercially available on the market [66].

Recently, Baeg et al. demonstrated ink formulation of n-type polymeric semiconductor ([poly{[N,N'-bis(2-octyldodecyl)-naphthalene-1,4,5,8-bis(dicarboximide)-2,6-diyl]-alt-5,5'-(2,2'-dithiophene)} [P(NDI2OD-T2), Polyera ActivInk N2200]. This together with two p-type polymers [P3HT and a dithiophene-based polymer (PolyeraActivInk P2100)] was used for ink-jet printing of top-gate/bottom-contact (TG/BC) organic field-effect transistors [67]. Anhydrous chlorobenzene (CB) was used as a solvent to obtain 0.5 mg/mL, 2.5 mg/mL, and 5 mg/mL semiconducting solutions for ink jet printing.

Figure 5 represents optical image of ejected droplets of P2100 and N2200 ink formulations respectively. For both formulations the diameter, volume, and velocity of these ejected droplets reported to be about 30–33 μm , 15–19 pL, and 3.0–3.6 m/s, respectively. The TG/BC organic field-effect transistors exhibit well-balanced and very-high hole and electron mobilities of 0.2–0.5 cm^2/Vs , which were enabled by optimization of the ink-jet printed active features, small contact resistance both of electron and hole injections, and effective control over gate dielectrics and choice of orthogonal solvent allowing to prevent electron trapping and semiconductor surface roughness. A combination of n- and p-channel conjugated polymers was employed to fabricate high performance polymer inverters (gain >30) and ring oscillators, having oscillation frequency ~50 kHz.

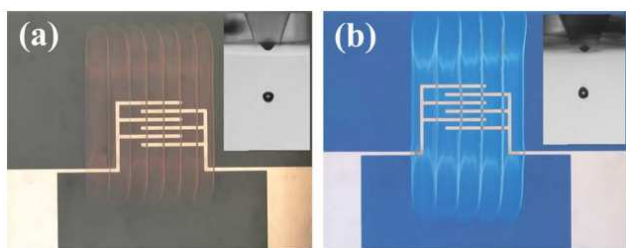


Fig. 5 Optical image of ink-jet-printed (a) P2100 and (b) N2200 TFTs and droplets (insets) (Reprinted from Journal of Polymer Science Part B: Polymer Physics, Vol. 49, K.-J. Baeg, D. Khim, D.-Y. Kim, S.-W. Jung, J. B. Koo, I.-K. You, H. Yan, A. Facchetti, Y.-Y. Noh, High speeds complementary integrated circuits fabricated with all-printed polymeric semiconductors, Pages No.62-67, Copyright (2010), with permission from John Wiley and Sons [67])

3.1.2. Metal based inks

Although significant progress has been made to improve the performance of polymers, metal based inks offer significant advantages in terms of conductivity. Conductive inks with metal

nanoparticles are widely studied and have attracted the attention of the scientific community [68]. For decades printable conducting metal inks that possess high conductivity and operational stability have been successfully applied in the form of nanoparticles for electronic circuits fabrication [69,70]. The market of conductive inks is forecasted to rise to \$3.36 billion in 2018, with \$735 million captured by new silver and copper nanostructure inks [71]. The metals of choice usually include silver, gold, copper and aluminium. Apart from their properties, the wide use of nanoparticles in inks is also related to the reduced size of the particles which in turn increases the surface to volume ratio and therefore promotes the increase in surface energy and reduction of melting point with respect to the bulk materials [72].

Fuller et al., suggested to use gold and silver nanoparticles dispersed in alfa-terpineol for ink-jet printing of electrically and functional metallic structures. The patterns were sintered at 300 $^{\circ}\text{C}$ to yield the resistivity of 3 $\mu\Omega\text{ cm}$, which is about twice of that for bulk silver [73]. Such solvents as isopropyl alcohol, ethanol, dodecane, toluene and butylbenzene were also reported to be used to form stable colloidal dispersions for ink-jet printing [74-80]. Lee et al. reported on silver nanoparticles of 7 nm in size were synthesized from silver nitrate using toluene. The dispersed nanoparticles in toluene were printed onto polyimide (PI) substrates, following the metallization at 250 $^{\circ}\text{C}$. The metallized silver patterns yielded resistance of 6 $\mu\Omega\text{ cm}$ [81]. However, it has been noted that use of volatile organic compounds (VOC) generally leads to the coffee-ring effect, i.e. the propensity for solute to deposit at the boundaries of a printed feature, which in turn hinders the quality of printed patterns. This fact has arisen the need in development of aqueous solution based inks. In the work of Lee et al., Ag- polyvinylpyrrolidone (PVP) stabilised nanoparticles were suspended in solvent mixture composed of water and diethylene glycol, which makes the process environmentally friendly with respect to use of toxic toluene and VOC containing solvents [81]. Coffee staining can be minimized in various ways such as printing onto a heated substrate as the material transfer to the contact line is reduced since the evaporation rate at all points on the deposited feature is increased; increasing the amount of solute or printing at high contact angle can also reduce coffee staining. It is reported that the use of a binary mixture of solvents in polymer solutions can eliminate the formation of ring stains if one of the solvents has a much higher boiling point than the other. Coffee staining is reduced as the solvent composition at the contact line shifts towards an increasing percentage of the higher boiling point solvent than in the bulk, which causes a decrease in the rate of evaporation at the contact line and establishes a surface-tension gradient [41].

However, the use of nanoparticle dispersion represents some limitations associated with particles themselves. First of all, in the case of ink-jet printing, particles define the nozzle diameters parameter of the ink-jet head and, therefore, minimal feature size of the patterns. Secondly, uniform and monodisperse nanoparticles are required to attain stable ink with reproducible performance as they have a high impact on the high dispersion stability and low electrical resistance at lower metallization temperatures [82,83]. Furthermore, the use of particles with a diameter larger than 5% of the nozzle diameter or aggregation of nanoparticles can promote clogging in the microfluidic system of the ink-jet head [17,84]. Moreover, the preparation of nanoparticles of inks often requires high energy input, high speed centrifuges or vacuum dryer thus making it difficult and expensive for mass production of inks [72].

To overcome these limitations the use of silver organic inks which represent an alternative to silver nanoparticle inks was suggested. This type of ink normally consists of the silver-organic material, the solvent and some additives. Dearden et al. reported the

formulation of ink based on a organic silver precursor, prepared by dissolving a synthesized silver carboxylate into a nonpolar organic solvent (xylene), for drop-on-demand ink-jet printer. They investigated resistivity as a function of temperature showing that conductivity values of $3.0\text{--}4.8 \times 10^{-8} \Omega\cdot\text{m}$, could be obtained at the temperature as low as 150°C with the same type of ink. [85]. In silver organic inks condensation and agglomeration don't occur as no particles are present, and the evaporation process is cost effective and simple. Note that the sintering step which involves the metal organic decomposition (MOD ink) and the evaporation of the organic compound often leads up to 90% volume loss [86,87]. Generally, depending on the mechanism used, silver organic inks can be divided into two groups, such as MOD ink and reduction ink. Jahn et al. demonstrated aqueous MOD ink based on a metal organic silver salt, namely silver (I) carboxylate, without additional stabilizing ligands. The ink was used for piezo ink-jet printing on PET substrates resulting in formation of electrically conductive layers having 18% of bulk silver conductivity and superior adhesion with respect to layers printed on inorganic substrates [88].

Chang et al. suggested to use silver-organic conductive ink with up to 30 wt% of silver content based on the reduction mechanism, where silver carbonate was used as the precursor, glycol as solvent and isopropyl amine as reducing agent [72]. The viscosity of the ink was reported to be 13.8 mPa·s and the surface tension was $36.9 \text{ mN}\cdot\text{m}^{-1}$, which makes it suitable for ink-jet printing. However, the ink was unstable in air. It was noted that to improve the stability of the ink water solvent and ammonia needed to be added to the formula, thus increasing the solubility of the complex.

Walker and Lewis reported on highly transparent reactive silver ink prepared by a modified Tollen's process for direct ink writing, ink-jet printing or airbrush-spraying. This ink benefits from low initial viscosity of 2 mPa·s, particle formation only after patterning and high conductivity (10^4 S/cm) at room temperature which makes it attractive for plastic electronics applications [89].

Another drawback of nanoparticle- based inks is related to the fact that printing of large area electronics by nanoparticle silver normally involves post-treatment procedures such as sintering or prolonged thermal treatment to achieve evaporation of organic stabilizers, densification of nanoparticles and the formation of continuous percolation network to produce required conductivity [88,90,91]. Such metallization represents a challenge since polymeric substrates have relatively low glass transition temperatures and limited thermal stability [88]. Therefore, an accurate time-applied temperature control is required at this stage because precursor materials must decompose before the substrate starts to soften or decompose [90]. Valetton et al. discussed a silver MOD ink which was reduced to silver by exposure to UV light and subsequent treatment with hydroquinone solution. Such room temperature treatment produced silver patterns having conductivity of 10% that of bulk silver and opens up possibilities to use low glass transition temperature polymeric substrates [92]. The sintering technologies also include microwave assisted sintering, electrical sintering plasma treatment and photonic sintering radiation [93].

Recently, Grouchko et al. reported a new conductive ink with built-in sintering mechanism containing 20 wt% silver nanoparticles, 10% propylene glycol and 0.05 wt% BYK 348 (BYK Chemie). The built in sintering mechanism (Fig. 6 (a)) was triggered during drying of the printed pattern and promoted high conductivity of 41% of bulk silver. The nanoparticles stabilized by a polymer underwent spontaneous self sintering due to the presence of a destabilizing agent, which came into action only during drying of the printed pattern. The destabilizing agent containing Cl^+ ions causes detachment of the anchoring groups of the stabilizer from the nanoparticles surface and thus enables their coalescence and

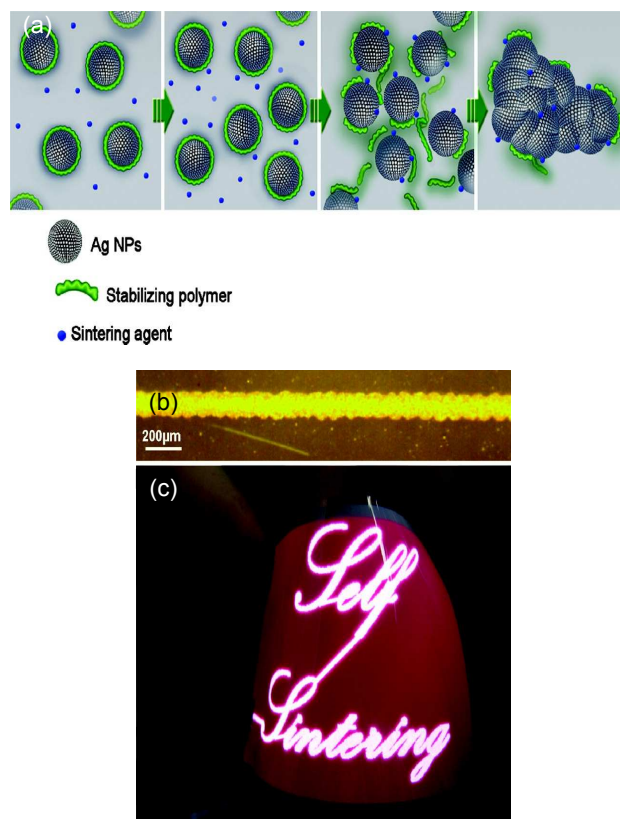


Fig.6 (a) Schematic illustration of the stabilizer detachment, which leads to the NP sintering (the green lines represent the polymeric stabilizer; the blue spheres represent the sintering agent), (b) Inkjet-printed line (the dispersion contained 20 wt % silver and 50 mM NaCl) on PET film and (c) electroluminescent device printed with the same dispersion composition. (Reprinted with permission from ACS Nano, Vol. 5, M. Grouchko, A. Kamyshny, C. F. Mihailescu, D. F. Anghel, and S. Magdassi, Conductive Inks with a "Built-In" Mechanism That Enables Sintering at Room Temperature, Pages No. 3354-3359, Copyright (2011), American Chemical Society [94])

sintering. The ink-jet printed pattern (Fig. 6(b,c)) was printed having $95 \mu\text{m}$ width and $0.5 \mu\text{m}$ thickness with the resistivity of $16 \mu\Omega\text{cm}$. Such method is promising for printing on heat-sensitive materials and in plastic printed electronics [94].

A particular effort is now being directed to study ways of reducing the width of tracks produced by inkjet printing. Thus, Van Osch et al. employing 1pL printhead produced lines of $40 \mu\text{m}$ wide on unstructured polyarylate, which had conductivity values of 13% that of bulk silver [70]. Meier et al., in turn, reported on $25 \mu\text{m}$ wide lines printed with 10pL printhead onto polyimide. They worked with ink, varying the temperature of print cartridge to decrease ink's viscosity and reduce the droplet size to 2pL by applying the low voltage [95].

Wu et al. reported a new binary hybrid silver nitrate ink, where silver nanowires were used as an additive to lower the concentration of silver nitrate. Silver nanowires increased the ink's viscosity and promoted fabrication of continuous and smooth silver lines with a resistivity of $7.31 \times 10^{-5} \Omega\text{cm}$ on a flexible Kapton substrate [96].

In order to reduce the cost attributed to the choice of noble metals such as gold and silver, mainly utilized in printing highly conductive elements, copper based ink formulation have been developed. Copper represents a good alternative to gold and silver due to its high conductivity and cost. Shultz et al. reported Cu(I)-

vinyltrimethylsilane and copper nanoparticles to direct write 5 μm thick lines with 2 Ω sheet resistivity on polyimide substrates [97]. The major drawback associated with the use of copper is its agglomeration and high ability to oxidation in ambient conditions [98, 99]. Modification of copper by organic polymers, alkene chains, amorphous carbon or graphene allows to increase the resistance to oxidation [100]. Jeong et al. reported on Cu nanoparticles dispersed in aqueous solutions of 2-methoxyethanol and glycerol. 2-methoxyethanol was introduced in order to adjust the surface energy of the aqueous ink to prevent the formation of satellites, while glycerol was used to control the evaporation rate to prevent the nozzle from clogging due to solvent evaporation along the nozzle orifice. The lines with narrow width of 45 μm , well controlled morphology, and resistivity of 11 $\mu\Omega\text{-cm}$ were ink-jet printed on polyimide substrates [100]. However, such approach might suffer from formation of a nonmetallic coating, requiring a selective reduction method. Grouchko et al. suggested to use transmetalation method to form 10-50 nm Cu-Ag core-shell nanoparticles based ink with tunable shell thickness [101]. Patterns having 300 μm width were obtained by ink-jet printing, while no oxidation and resistivity greater than $3.0 \times 10^4 \mu\Omega\text{cm}$ was observed after heating at 150° C.

However, low interfacial reactivity may result in poor mechanical properties of conductive features on polymeric substrates such as polyimide. Lee and Choa reported on copper complex ion-based ink-jet ink containing a silane coupling agent to promote better adhesion to the polyimide. The polyimide substrate was treated with oxygen plasma, and the chemical reaction between the 3-aminopropyl-trimethoxy-silane (APS) in the ink and the polyimide surface was enhanced by increasing the number of hydrophilic groups. The rectangular form of patterns (3 cm x 8 cm) and complex lines with a width of 100 μm were successfully created by an ink-jet printing process on the oxygen plasma-treated polyimide using copper complex ion ink with varied APS content. In this case, the increase of silane additive resulted in diameter increase of the droplet along with the decrease of contact angle. The presence of silane also promoted the increase of resistivity of printed features up to 24.3 times higher than that of the bulk copper after sintering at 200 °C. This phenomenon is related to the increased porosity in the pattern and the presence of residual silicon [102].

3.1.3. Carbon based inks

Carbonaceous materials, such as carbon nanotubes (CNT) and graphene, represent an alternative conducting material and have been recently considered for the printable semiconductive layers and transparent electrodes [103]. This is attributed to their unique properties including high mechanical strength, high stability, high transparency, good compatibility with organic semiconductors and low-cost [104].

Carbon nanotubes represent sheets of graphene bent into a cylindrical shape and exist as a single walled nanotube (SWCNT) and as a multiwalled nanotube (MWCNT). State of the art states that SWCNT yields mobility of 100 000 $\text{cm}^2 \text{V}^{-1}\text{s}^{-1}$ [105], conductivity of 400 000 $\text{S}\cdot\text{cm}^{-1}$ and tube diameter dependent band gap. Note that depending on chirality CNTs can exhibit either metallic or semiconducting behaviour.

While developing CNT ink formulations several factors have to be taken into consideration such as material quality, ink stability and degree of nanotubes dispersion. A major challenge of research in the fabrication of transparent conductive films is the formulation of purified CNT material into printable inks. However, the solubilization of CNTs in water and other polar solvents is restricted due to the non polar nature of CNTs and high affinity between the tubes determined by a strong Van der Waals interaction

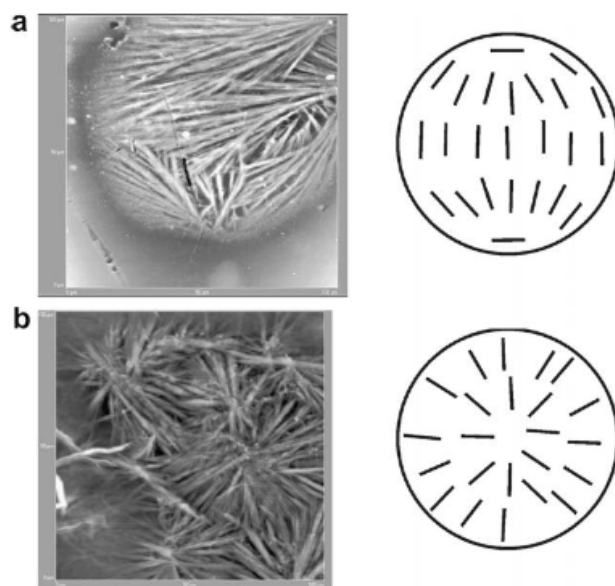


Fig. 7 AFM image of 100 $\mu\text{m} \times 100 \mu\text{m}$ area of a single ink-jet-printed film of SWCNTs on (a) a polyester substrate and (b) polyester treated with PEI. The figures on the right depict the possible configurations of a polymer dispersed liquid crystal. The directors are shown as lines, with respect to the polymer surface: top parallel alignment; bottom perpendicular alignment. (Reprinted from Carbon, Vol. 47, M.F. Mabrook, C. Pearson, A.S. Jombert, D.A. Zeze, M.C. Petty, The morphology, electrical conductivity and vapour sensing ability of inkjet-printed thin films of single-wall carbon nanotubes, Pages No. 752-757, Copyright (2009), with permission from Elsevier [113])

[106]. Therefore, one of the major challenges in fabricating a CNT film is to separate the tubes, without using covalent chemistries or other harsh conditions, which could lower their electrical conductivity. Moreover, ink-jet printing of carbon nanotube formulations can only be achieved with water or alcohols, to avoid damaging of polymer printer components by organic solvents [107]. Major approaches to disperse CNT include dispersing CNTs in neat organic solvents or superacids, dispersing CNTs in aqueous media with the use of dispersing agents such as surfactants, dispersants, or other solubilization agents or functionalization of CNTs [108].

Kordas et al. demonstrated water based ink-jet ink of functionalized multiwall carbon nanotubes. The functionalization was conducted by refluxing MWCNTs in nitric acid to produce carboxyl, hydroxyl and carbonyl functional groups at the defect sites of the outer graphene layer of the nanotubes. Due to high surface tension of the ink the dispersed droplets did not spread on the surface as much as ordinary dye ink, and lines having width of 70 μm were printed. Multiple layer printing resulted in formation of prints having sheet resistivity of 40 $\text{k}\Omega/\text{cm}$ which did not need curing to be conductive [109]. However, covalent functionalization strategies suffer from defects in nanotube sidewalls and shorten SWCNTs via oxidative cutting [110]. To overcome this drawback Trevor et al. reported on SWCNTs dispersed in water by noncovalent modification of the tube surfaces with polymers, i.e. polyvinylpyrrolidone, and a sodium dodecyl benzene sulfonate (SDBS) used as a surfactant aided by low-power sonication. The black ink solution contained 0.1 wt% SWCNTs in suspension. This method allows to achieve high concentrations of SWCNTs dispersed in water and hinders damaging of SWCNTs [111].

Mabrook et al. demonstrated the use of sodium dodecyl sulphate (SDS) stabilized SWCNT based aqueous solution for sensor fabrication by ink-jet printing. The ink viscosity was adjusted by addition of up to 20% of ethylene glycol. Note, SDS is often used

surfactant to provide a satisfactory degree of separation among the bundles of nanotubes [112]. When a surfactant wraps nanotube agglomeration, the cluster would break up into smaller aggregations. The as-prepared ink was printed on polyester and poly(ethyleneimine) (PEI) coated polyester substrates forming printed films containing long bundles of nanotubes having the lengths of up to 80 μm , orientation of polymer liquid crystal is believed to be attributed to the substrate nature (Fig. 7). Better coverage and reduction of nanotube islands in size from 100 to 45 μm for modified substrates was also observed [113].

Beecher et al. reported on surfactant free composition of CNT ink having final concentration of CNT of 0.003 mg/mL, where HiPCO CNT were dispersed in N-methyl-2-pyrrolidone. The solution was centrifuged and filtrated to make sure that no CNT agglomerates are present, which allowed ink-jet printing without clogging the printhead [114].

Recently, Kim et al. [115] demonstrated formulation of hybrid inks for the channel material in TFT consisting of SWCNTs and a polymer semiconductor, poly(didodecylquaterthiophene-alt-didodecylbithiazole) (PQTBTz-C12), which was designed to improve the molecular order of the polymer, and to modulate the interaction with the semiconducting SWCNTs without charge transfer. The printed films exhibited high mobility of 0.23 $\text{cm}^2/(\text{V}\cdot\text{s})$.

Another limitation for using SWCNTs in nano- or microelectronic applications is the lack of a manufacturable process to precisely assemble SWCNTs into small devices. The two main challenges facing CNT include the difficulty of placing and aligning CNTs over large areas and low on/off current ratios due to admixture of metallic nanotubes, preventing their applications in a wide variety of commercial settings [116]. A complete study of the relationships between density, mobility, on-off ratio and purity of CNT inks was provided elsewhere [116].

Graphene is another carbonaceous material, that has recently emerged as an environmentally stable electronic material with exceptional thermal, mechanical, and electrical properties because of its two-dimensional sp^2 bonded structure [117-121]. In particular, high specific surface area of graphene and its high charge carrier mobility makes it an attractive candidate for electrode fabrication [122]. Just like graphene, graphene oxide (GO) has very high specific surface area. Although graphene oxide has a low electrical conductivity, it can be thermally, chemically and photothermally reduced to increase electrical sheet conductance to levels comparable to those achieved with pristine graphene films [123-125]. Therefore, it is anticipated that ink-jet-printed and thermally reduced graphene oxide may serve as conformal, scalable and economically viable supercapacitor electrodes, particularly for flexible energy storage devices, sensing electrodes, in miniature power applications etc. [126].

Recently, graphene based inks were prepared by sonicating single-layered and few-layered graphene produced by modified Hummers method in water. It is crucial to restrict the size of graphene materials in order to obtain high quality prints and printhead reliability, therefore centrifuge was used to remove large sized particles of graphene material and the suspension was further filtered through the filter with 0.45 μm pore size [127]. Ink-jet printing was conducted on modified PET and PI substrates, followed by thermal reduction at temperatures up to 400 $^\circ\text{C}$. The obtained patterns yielded high conductivity and flexibility and are promising for application in solar cells, sensors, FET.

Torrisi et al. also reported ink fabrication via liquid phase exfoliation (LPE) of graphite flakes in N-methylpyrrolidone, the obtained solution was ultracentrifuged and filtered to remove the flakes $> 1\mu\text{m}$ to avoid clogging while printing [128]. The ink was used to print thin film transistors with mobilities up to 95 $\text{cm}^2/(\text{V}\cdot\text{s})$.

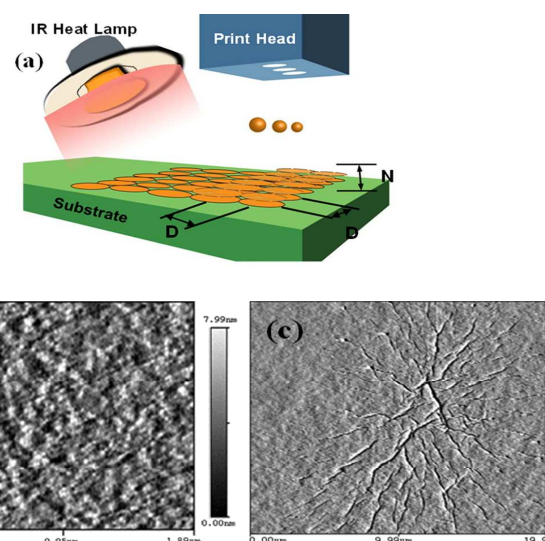


Fig. 8. a) Illustration of inkjet-printing of GO sheets and photothermal reduction using IR heat lamp (where D is spacing between adjacent ink droplets and N is the number of printed layers), b,c) AFM images of dried-out structures produced by a single GO ink droplet. (Reprinted with permission from Langmuir, Vol. 28, D. Kong, L.T. Le, Y. Li, J. L. Zunino, and W. Lee, Temperature-Dependent Electrical Properties of Graphene Inkjet-Printed on Flexible Materials, Pages No. 13467–13472, Copyright (2012) American Chemical Society. [129])

Kong et al. [129] recently reported on inkjet printing of graphene oxide sheets dispersed in water (2mg/mL) on polyethylene terephthalate and Kapton substrates followed by infra red reduction (Fig. 8 (a)). Dried out structure allowed the coffee ring formation. As a result of pinning at the edge of the low contact angle area of the droplet, most GO sheets appeared to clump and form aggregated structures 5-10 nm high and 100-200 nm wide at the perimeter (Figure 8 (b)). Star-shaped assembly of nanoscale features at the center region of the droplet was observed (Figure 8 (c)), while leaving a significantly lower number of sheets scattered between the center and the perimeter regions of 10-20 nm and 50-200 nm, respectively. As the evaporation front receded toward the center of the shrinking droplet, it appeared that the droplet became depinned and the GO sheets become entrained, accumulated, and eventually deposited to form the star-shaped assembly at the center region of the droplet. Scrutinizing the spacing between adjacent ink droplets (D) and the number of printed layers (N) as two major process parameters suggested that $D=20\text{ mm}$ and $N=5$ was adequate spacing to promote continuous morphology, moreover increasing in N and decreasing D led to the reduction of resistivity up to 0.3MW and transparency of 86% of fabricated graphene electrodes associated with formation of continuous morphology and allowing electron transport paths.

Despite CNT and graphene inks have been recently used in flexible electronics several issues still need to be addressed with regard to ink-jet-printing these nanomaterials for practical applications. CNT and graphene suffer from: high costs, lack of commercial availability in large quantities, tendency to aggregate in pure water due to their hydrophobic nature. The addition of surfactants can increase the stability of CNT and graphene dispersion, but most surfactants are found to have detrimental effects on capacitance. Moreover, there is a need in reducing drying times the both for conventional and digital printing techniques, this will strongly affect the final SWNT density as well as mobility. Heating during printing which can be employed to aid this process may,

however, be undesirable in case of plastic substrates and cause damaging. Finally, more research should be done in depositing inks onto plastic substrates such as polyimide and polytetrafluoroethylene, and in systematic comparison with competing, lower-mobility inks for each application [126].

3.2. Insulating materials formulation

Despite polymers have lower dielectric constant values than inorganic dielectrics [130,131], polymer insulating layers have been widely studied [7,132-136]. Polymer dielectrics advantages are associated with good insulating properties and high intrinsic breakdown voltage; they can undergo plastic deformation when external stress is applied, thus reducing residual stress in the dielectric films; most polymers are solution processable by spin-coating or printing; they also provide smooth films on transparent glass and plastic substrates; are suitable for optoelectronics like photoresponsive OFETs owing to their high optical transparency, and can be thermally stable up to 200 °C with a relatively small thermal-expansion coefficient [137,138]. As far as polymeric insulators are concerned, polyvinylphenol (PVP) [40], polystyrene (PS) [30], polyimide [139,140], sol-gel derived siloxane based hybrid polymer [141], polyester [56], polymethylmethacrylate [142], polyvinylalcohol [143], poly(vinyl pyrrolidone) [144] are widely used due to its broad and complementary solubility, processability and dielectric properties [102, 145, 146]. The insulator materials play a crucial role in electronic devices; Facchetti et al reviewed dielectric materials and deposition techniques used for these materials elsewhere [145].

Ultra thin polymer dielectric insulators have been investigated for low-voltage operation applications. Accordingly, polymer cross-linking has been proven to be efficient to enhance ultra thin film uniformity and to prevent large leakage current along with film thickness decrease due to the pinholes and defects [134]. The presence of hydroxyl reactive groups in such polymers as polyvinylalcohol (PVA) and PVP allows them to react with various commercially available and moisture sensitive crosslink additives [147 -151]. PVP is a widely used polymer dielectric, because of its easy rheological tunability, good insulating performance and relatively low -temperature thermal curing condition [152-154]. Yoon et al reported on the use of various organosilane cross-linking agents blended with PS and PVP, the as-prepared mixture was spin coated into a ultrathin (10-20 nm), uniform, smooth and pinhole free dielectric layers with a controllable thickness [151].

Jeong et al. reported hybrid organic-inorganic sol-gel derived methyltriethoxysilane and tetraethylorthosilicate dielectric. In order to prepare the ink-jet ink the solid precursor (~1 wt%) was mixed with various solvents including ethylene glycol, 1-propanol, 2-methoxyethanol, while for spin coating it was diluted with ethyl lactate, stirred to form homogeneous dispersions and filtered through a membrane filter [155]. The deposition was carried on Si substrates, followed by annealing at 190 °C in order to evaporate the solvent. It was noted that the ink based on a single solvent of 1-propanol tended to clog the nozzle and prevented a uniform ejection of the droplets due to relatively rapid solvent evaporation. In this case stable jetting property was obtained by adding high boiling point co-solvent, i.e. ethyleneglycol. However, the dot-shaped dielectric film exhibited significant coffee ring effect along with surface tension gradient resulting in Marangoni flow. Substitution of ethyleneglycol for 2-methoxyethanol allowed to diminish the outward Marangoni flow by decreasing the surface tension difference and, in turn, minimizing the coffee ring effect. It was observed that the leakage current through the printed dielectric is less than 10^{-6} A/cm² until a bias of 90 V is applied, and the dielectric constant of printed dielectric is

4.9. In addition, it was confirmed that the ink-jet-printed dielectric layer performs electrically similarly to their spin-coated counterparts. However, the residual solvent molecules induced a large hysteresis behavior and positive shift of the threshold voltage for the printed dielectric- based organic transistor.

Kang et al. studied [27] dielectric layer obtained by microgravure printing of poly-4-vinylphenol (7.6 wt%) dissolved in 1-hexanol. Note, PVP exhibits shear-thinning behaviour with viscosities varying from 10 cP to 500 cP by adjusting polymer concentration. The viscosities ~100 cP were required to obtain clear square prints with well-defined edges without film break-up, no pinholes. It was found that along with high viscosities, high printing speed was required to improve the printability as it led to the increase of capillary number of the ink. It was also noted that smoothness of the conductive underlayer is critical for endurance of dielectric layer built upon it. PVP capacitors printed on the silver metal lines show very low leakage current density $1 \mu\text{A}\cdot\text{cm}^{-1}$ at $2\text{MV}\cdot\text{cm}^{-1}$. Ko et al also reported on dielectric formation employing PVP dissolved in hexanol and propylene glycol monomethyl ether acetate (PGMEA) by spin-coating and ink-jet printing respectively [40,156]. Halik et al. reported gate dielectric layer, having thickness of 440 nm and average surface roughness of 7 Å, prepared from a solution of poly-4-vinylphenol and polymelamine-co-formaldehyde methylated in n-butanol, deposited by spin coating and cured at 200 °C. Gate leakage was on the order of 5 mA/cm² at a gate bias of 20 V and permittivity was estimated at 4.2, related to the molecular ordering in the organic active layer, and in turn, improved charge transport and carrier mobility, due to smooth gate dielectric [157].

In case of ink-jet printing PVP solution jetting conditions should be optimized to obtain a well-defined gate dielectric layer because PVP solvent can easily result in cartridge nozzle clogging [154]. Chung et al reported on the use of poly(melamine-co-formaldehyde) as a cross-linking agent for PVP dissolved in propylene glycol methyl ether acetate. It is suggested that PVP and cross-linking agent concentrations determines viscosity of the PVP solution and insulation and surface energy property of the printed films and are also critical factors to make a spherical shape of ink droplets which help forming a well-defined gate dielectric layer. PVP solution was ink-jet-printed at room- temperature in order to prevent fast solvent evaporation which was found to degrade the quality of the printed film. Drop spacing of 25 μm and two times printing was used for uniform 1μm dielectric film formation to optimize film quality and leakage current behavior.

Recently, ink jet printing of ion-gel dielectric material was demonstrated for dielectric applications in printable organic electronic circuits [158]. Cho et al. developed the material representing a mixture of an ionic liquid and triblock copolymer. Upon solvent evaporation, the triblock copolymer assembled into a network-like gel filled with ion-liquid. Due to relatively large conductivity of the ion liquid, transistors based on this ion-gel dielectric layer can be switched in a frequency as large as 10 kHz which makes it promising for applications in low-end radio displays and e-books.

More recently, graphene oxide has been employed as a gate dielectric for graphene-based thin film transistors due to its good mechanical and optical properties and ease of fabrication from solution- or direct oxidation methods at room temperatures [159-161]. Lee et al. exploited graphene oxide dielectrics [162] in all-graphene based TFT. In particular, the two-dimensional films were formed from GO flakes in aqueous phase stabilized by the negatively charged functionalities. An immiscible water/oil interface was formed by pouring hexane on the water surface, and ethanol was then added slowly to the surface of the water/hexane layer by using a mechanical syringe pump, resulting in GO trapping at the interface.

The dielectric constant of water decreases when a miscible solvent with a lower dielectric constant, such as ethanol, is added. Adding of ethanol led to gradual decrease in the surface charge of the GO flakes. The decrease in interfacial energy at the water/hexane interface by the adsorption of GO flakes is thought to be the driving force for the entrapment of GO flakes, as the charge separation ability of water is reduced by the ethanol addition. The spontaneous evaporation of hexane leaves the two-dimensional GO films floating on the top of the water surface. Sparsely floating GO flakes can be assembled into one large close-packed film by decreasing the surface area using two Teflon bars. The close-packed GO films could then be transferred by horizontal lifting to a substrate. Finally we stacked pinhole-free multilayered GO structures by repeating the Langmuir-Blodgett (LB) method. The as deposited graphene oxide films exhibited dielectric constant of 3.1 at 77 K, and the leakage current density was 17 mA/cm² at a bias field of 50 MV/cm.

3.3. Printing of biological active layers

Patterning inks aren't limited to plastics and metals. There is a growing interest in printing biomaterials such as proteins, cells and tissues [163-165]. For instance, proteins are widely used as building blocks for fabrication of functional materials. Immobilization of biomolecules onto solid supports usually consists of two steps. First, the bioagent is delivered onto the surface. In the second step immobilization of protein itself occurs. Note that the nature of the substrate determines if bioagent interacts with the support via physisorption or covalent bonding [166].

In perspective of developing innovative, low-cost, small-volume, solution-based screening methods [167] it is necessary to address biological ink formulation problem. In this case we should take into account not only its physico-chemical properties to make ink stable and ejectable, but also preservation of its biological functionality [168]. Therefore, an accurate selection of ink additives, printing operation conditions and viscosity modifiers is crucial to maintain enzyme activity and avoid its denaturation.

A number of solution based techniques have been used to deposit biomaterials onto solid surfaces including microcontact printing, ink jet printing and dip pen nanolithography. Sumerel et al. demonstrated microscale patterning of several biological materials, including streptavidin protein, monofunctional acrylate ester, sinapinic acid, DNA, and DNA scaffolds [169]. Di Risio et al. using piezoelectric ink jet printer deposited a bioink containing horseradish peroxidase using various viscosity modifiers including PEG, ethylene glycol, PVA, CMC on solid surfaces [168]. Setti et al. reported on bioink formulation containing Glucose oxidase (GOD) from *Aspergillus niger* in phosphate buffer, pH 6.5. Additives used included tetrasodium salt hydrate (EDTA) as antimicrobial agent and glycerol as stabilizer [170]. Inhere, glycerol acts as a wetting agent, to avoid the clogging effect on the external nozzle surface. Furthermore glycerol is reported to increase the enzyme stability to the thermal shock, by means of interactions between the polyol and the protein [171]. The obtained ink was used to fabricate electrochemical biosensor by thermal ink-jet printing biological ink on PEDOT:PSS prepatterned ITO-coated glass substrates yielding resolution of 221×221 dpi with no significant differences in the enzyme activity [170].

Arrabito et al. studied jettability and spreading behaviour at the solid surface while printing glucose oxidase onto silicon oxide substrates. In this case biological ink containing from 0% to 50% of glycerol as an additive was printed using piezo-based ink-jet print cartridges, each with 16 nozzles 254 μm spaced and 21.5 μm in diameter. It was observed that increasing glycerol content in ink formulation up to 50% and, therefore, higher ink viscosity promoted

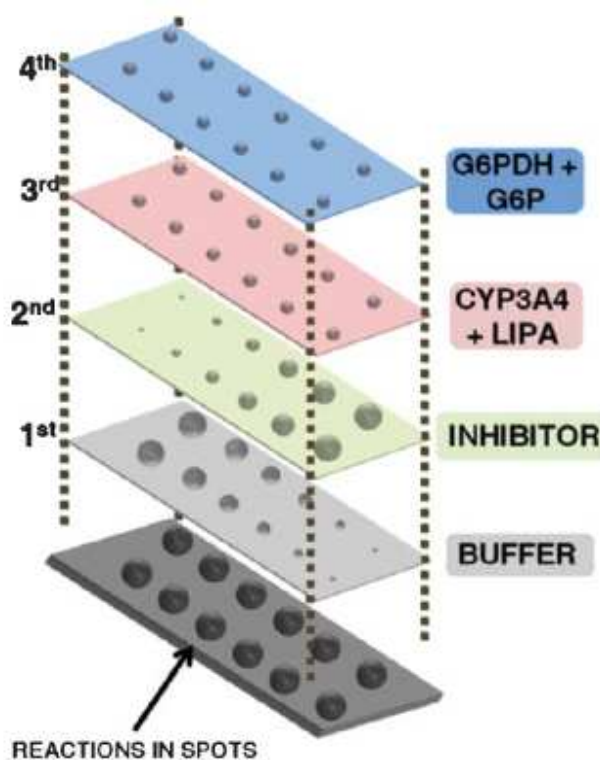


Fig. 9 Layer-by-layer fabrication of enzymatic assay. Reproduced from Ref. 174 with permission from The Royal Society of Chemistry

the formation of high quality defined patterns, consisting of circular well-aligned drops having size of 30.2-31.3 μm along with the retaining of the biological activity [172].

The same approach to optimise viscosity and surface tension was employed to print D-glucose or a mixture of D-glucose/D-glucal onto a glucose oxidase monolayer immobilized on a silicon oxide surface [173]. This method however required the need of covalent bond between the macromolecules and solid support. To overcome this limitation Arrabito et al. developed printing of multiple biomolecular systems (Fig. 9) in a multi step sequential picoliter droplets (water glycerol) assembly on solid surfaces. Addition of glycerol (characterised by high hygroscopicity) at 30% allowed to keep liquid spots stable during both the multilayer detection and the execution of the assay [174].

Another important field for printing in bio-organic electronics is concentrated on printing of cells. Recently, Ferris et al produced new bio-ink formulation by microgel suspension in a standard cell culture media using the low viscosity biopolymer - gellan gum [175]. For the first time they reported the use of surfactants to reduce surface tension whilst maintaining the biocompatibility of the bio-ink. The surfactants included the non-ionic polymeric surfactant Poloxamer 188 (P188), which is an established medium additive often used for protecting cells from fluid-mechanical damage, and non-ionic polymeric fluorosurfactant Novec FC-4430, which exhibit both greater surface activity and lower cytotoxicity than their hydrocarbon analogues. Such bio-inks display optimal fluid properties allowing printing multiple cell types over long periods, preventing cell settling and allowing controlled deposition of cells. This innovation may pave the way to the fabrication of multi-cellular and/or larger structures.

Conclusions

Printed electronics represents today's an emerging field of electronics allowing for alternatives or new and different applications with respect to silicon based technology. It is well known that traditional silicon-based technology typically requires high process temperatures while molecular based devices can usually be manufactured at or near room temperature, and thus on flexible polymeric substrates and even on a paper. In this context, solution processing techniques allow to achieve efficient new materials resulting in fabrication of new active layers for emerging technologies.

In this review we focused on the printing techniques that are most relevant to the field of PE such as gravure printing, screen printing and ink-jet printing techniques. In the related field of plastic electronics, solution printing techniques were used to fabricate solar cells, organic light emitting diodes, field effect transistors, organic thin film transistors etc. Notably, screen printing yields patterns with high thickness and relatively low resolution 75 μm , while gravure printing exhibits resolution up to several nanometers with high throughput speed of up to 1m/s. In case of ink-jet printing the resolution of printed patterns is comparable to the nozzle diameter and typically is 30-100 μm . However careful optimization of nozzle size is required, as it reduces the window of inks that can be used for printing depending on the viscosity and surface tension.

Despite the impressive progress in the development of plastic electronics devices, the promise of solution patterning techniques has not been fully fulfilled, and there are still many challenges and obstacles related to the achievement of a highly stable and reliable, high throughput patterns with good resolution. Clearly the successful development of printable electronics, to be flanked to the silicon-based one, depends on the development to new materials and new material interfaces, as well as on the multidisciplinary understanding and partnerships among chemists, physicists and engineers. Yet, the ultimate implementation of the new devices may rely on knowledge transfer from scientific lab to develop commercially viable large-scale production processes.

The review also highlights synthesis and properties of ink formulations applied in the field. As already mentioned, ink properties such as viscosity and volatility are associated with the printing technique itself while some of the properties relate to the interaction of the ink with the substrate surface [30]. Hence, further developments in materials, electronic properties and chemical functionalization will continue to impact the PE field. Therefore, a careful optimization of ink properties and formulation is required depending on the chosen printing technique and device material application.

Conducting polymers related to PE applications have recently become an important topic in scientific research and R&D demonstrating great processing versatility. Some important p-type conducting polymers, such as polythiophenes and their copolymers were widely studied due to many advantages such as charge transport, rheological and mechanical properties. It is clear that the field of n-type semiconductor polymer inks is still under development, and requires the formulation of easily processable, therefore, soluble polymers to realize high-performance, although ambient-stable n-channel polymeric semiconductors yielding charge transport efficiencies close to p-channel polymers have been already realized.

The review also shows the use of polymers as insulating layers, whereby the control over the structure by cross-linking is efficient to enhance layers uniformity and allows good thickness control resulting in pin-hole and defect free morphologies. Moreover, the choice of the solvent plays a significant role in uniform drop ejection and nozzle clogging protection like in case of

ink-jet printing. Therefore, the use of solvents decreasing the surface tension difference and, in turn, minimizing the coffee ring effect is favored. Recently, the use of ion-gels and graphene oxide materials has been demonstrated as an alternative to polymer dielectric materials suggesting a promising route to create good electrical, optical, and mechanical performance for plastic electronic applications which would be difficult to achieve using conventional electronic materials.

The important advantage of using metal nanoparticles based inks, as opposed to semiconducting polymers is also demonstrated. The efforts here should be focused on minimizing the feature size of the printed patterns as well as to avoid the nozzle clogging by careful control over nanoparticles dimensions. Moreover, an optimization of formulation-processing-sintering is required to maintain the dispersion stability, and the electrical resistance of the printed patterns. In this respect, self-sintering mechanisms, where sintering occurs spontaneously due to the presence of a destabilizing agent, are attractive.

As to carbon based inks containing carbon nanotubes and graphene oxide, they have shown the promise for printing of semiconducting active layers and electrodes. Despite their outstanding electrical and mechanical properties the main difficulties in using carbonaceous based inks are obtaining purified CNT material with high quality, good stability and degree of dispersion and, difficulty of placing and aligning CNTs over large areas, size control over graphene molecules to avoid clogging while printing, high cost and long drying times.

As far as it concerns printing of bioactive phases, an accurate choice of solvents is required to trigger the viscosity of the ink, its stability and drying properties after printing as well as maintaining the biological functionality of the materials to allow fabrication of complex 2D-3D patterns and multiple assays.

To sum it up, future R&D efforts should be spent on the development of inks for thin-film absorber layers, dielectric materials, transparent conductors, and metal contacts, in combination with solution deposition and processing techniques to provide a simple, low cost, energy efficient, low temperature sintering, environmentally friendly and roll-to-roll compatible processing to produce structures with high resolution.

Acknowledgements

Italian MiUR is acknowledged for funding through FIRB - Futuro in Ricerca (RBFR08DUX6) and FIRB-MERIT (RBNE08HWLZ_010), PON R&C 2007-2013 ("TESEO" - PON02_00153-2939517 and "Plastic electronics for smart disposable systems" - PON02_00355 - 3416798).

Notes

^a Dipartimento di Fisica e Chimica, Università degli studi di Palermo, V.le delle Scienze-Parco D'Orleans II, ed. 17-90128 Palermo, Italy. *Corresponding author e-mail: bruno.pignataro@unipa.it

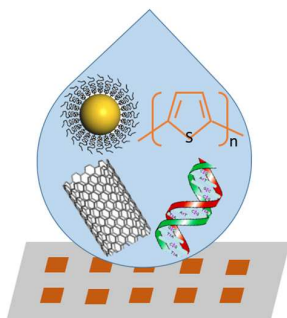
References

1. D. Gentili, P. Sonar, F. Liscio, T. Cramer, L. Ferlauto, F. Leonardi, S. Milita, A. Dodabalapur, and M. Cavallini, *Nano Lett.*, 2013, **13**, 3643.
2. A.C. Arias, J.D. MacKenzie, I. McCulloch, J. Rivnay and A. Salleo, *Chem. Rev.*, 2010, **110**, 3.
3. S. Cataldo and B. Pignataro, *Materials*, 2013, **6**, 1159.
4. M. Cavallini, I. Bergenti, S. Milita, J. C.n Kengne, D. Gentili, G. Ruani, I. Salitros, V. Meded, and M. Ruben, *Langmuir*, 2011, **27**, 4076.

5. M. Cavallini, P. D'Angelo, V. V. Criado, D. Gentili, A. Shehu, F. Leonardi, S. Milita, F. Liscio and F. Biscarini, *Adv. Mater.*, 2011, **23**, 5091.
6. M. Cavallini, *J. Mater. Chem.*, 2009, **19**, 6085.
7. T.B. Singh and N.S. Sariciftci, *Annu. Rev. Mater. Res.*, 2006, **36**, 199.
8. H.E. Katz and J. Huang, *Annu. Rev. Mater. Res.*, 2009, **39**, 71.
9. S. Fabiano and B. Pignataro, *Chem. Soc. Rev.*, 2012, **41**, 6859.
10. *Printed Organic and Molecular Electronics*, ed. D.R. Gamota., P. Brazis, X. Kalyanasundaram and J. Zhang, Kluwer Academic Publishers Group, New York, 2004, pp. 1-705.
11. H. Sirringhaus, *Nat. Mater.*, 2003, **2**, 641.
12. J. Granstrom and H.E. Katz, *J. Mater. Res.*, 2004, **19**, 3540.
13. M. Shtein, P. Peumans, J.B. Benziger and S.R. Forrest, *Adv. Mater.*, 2004, **16**, 1615.
14. A. Knobloch, A. Manuelli, A. Bernds and W. Clemens, *J. Appl. Phys.*, 2004, **96**, 2286.
15. W. Fix, A. Ullmann, J. Ficker and W. Clemens, *Appl. Phys. Lett.*, 2002, **81**, 1735.
16. H. Yan, Z. Chen, Y. Zheng, C. Newman, J.R. Quinn, F. Do and A. Facchetti, *Nature*, 2009, **457**, 679.
17. J. Park and J. Moon, *Langmuir*, 2006, **22**, 3506.
18. Y.I. Lee and Y.H. Choa, *J. Mater. Chem.*, 2012, **22**, 12517.
19. J.Z. Wang, Z.H. Zheng, H.W. Li, W.T.S. Huck and H. Sirringhaus, *Nat. Mater.*, 2004, **3**, 171.
20. *US Pat.*, 4765243, 1988.
21. M. Lahti, S. Leppavuori and V Lantto, *Appl. Surf. Sci.*, 1999, **142**, 367.
22. J.M. Ding, A. De La Fuente Vornbrock, C. Ting and V. Subramanian, *Sol. Energy Mater. Sol. Cells*, 2009, **93**, 459.
23. P. Kopola, T. Aernouts, S. Guillerez, H. Jin, M. Tuomikoski, A. Maaninen and J. Hast, *Sol. Energy Mater. Sol. Cells*, 2010, **94**, 1673.
24. P. Kopola, T. Aernouts, R. Sliz, S. Guillerez, M. Ylikunnari, D. Cheyins, M. Välimäki, M. Tuomikoski, J. Hast, G. Jabbour, R. Myllylä and A. Maaninen, *Sol. Energy Mater. Sol. Cells*, 2011, **95**, 1344.
25. X. Yin and S. Kumar, *Chem. Eng. Sci.*, 2006, **61**, 1146.
26. M. Pudas, J. Hagberg and S. Leppävuori, *Prog. Org. Coat.*, 2004, **49**, 324.
27. H. Kang, R. Kitsomboonloha, J. Jang and V. Subramanian, *Adv. Mater.*, 2010, **24**, 3065.
28. M.M. Voigt, A. Guite, D.Y. Chung, R.U.A. Khan, A.J. Campbell, D.D.C. Bradley, F. Meng, J.H.G. Steinke, S. Tierney, I. McCulloch, H. Penxten, L. Lutsen, O. Douheret, J. Manca, U. Brokmann, K. Sonnichsen, D. Hulsenberg, W. Bock, C. Barron, N. Blanckaert, S. Springer, J. Grupp and A. Mosley, *Adv. Funct. Mater.*, 2010, **20**, 239.
29. R. Søndergaard, M. Hösel, D. Angmo, T.T. Larsen-Olsen and F.C. Krebs, *Mat. Today*, 2012, **15**, 36.
30. F.C. Krebs, *Sol. Energy Mater. Sol. Cells*, 2009, **93**, 394.
31. P.F. Moonen, I. Yakimets and J. Huskens, *Adv. Mater.*, 2012, **24**, 5526.
32. E. Menard, M.A. Meitl, Y. Sun, J.U. Park, D.J.L. Shir, Y.S. Nam, S. Jeon and J.A. Rogers, *Chem. Rev.*, 2007, **107**, 1117.
33. F.C. Krebs, *Sol. Energy Mater. Sol. Cells*, 2009, **93**, 465.
34. C. Xia, F. Chen and M Liu, *Solid State Lett.*, 2001, **4**, A52.
35. D. Zielke, A.C. Hübler, U. Hahn, N. Brandt, M. Bartzsch, U. Fügmann, T. Fischer, J. Veres and S. Ogier, *Appl. Phys. Lett.*, 2005, **87**, 123508.
36. C. Gray, J. Wang, G. Duthaler, A. Ritenour and P.S. Drzaic, Proc. SPIE4466, Organic Field Effect Transistors, San Diego, 2001.
37. S.E. Shaheen, R. Radspinner, N. Peyghambarian and G.E. Jabbour, *Appl. Phys. Lett.*, 2001, **79**, 2996.
38. Y. Wen, Y. Liu, Y. Guo, G. Yu and W. Hu, *Chem. Rev.*, 2011, **111**, 3358.
39. B.J. De Gans, P.C. Duineveld and U.S. Schubert, *Adv. Mat.*, 2004, **16**, 203.
40. S.H. Ko, J. Chung, H. Pana, C.P. Grigoropoulos and D. Poulikakos, *Sensor Actuat. A-Phys.*, 2007, **134**, 161.
41. E. Tekin, P.J. Smith and U.S. Schubert, *Soft Matter*, 2008, **4**, 703.
42. J. Moon, J. E. Grau, V. Knezevic, M.J. Cima and E.M.J. Sachs, *Am. Ceram. Soc.*, 2002, **85**, 755.
43. R. Parashkov, E. Becker, T. Riedl, H.H. Johannes and W. Kowalsky, *Proc. IEEE*, 2005, **93**, 1321-1329.
44. T. Kawase, S. Moriya, C. J. Newsome and T. Shimoda, *Jpn. J. Appl. Phys.*, 2005, **44**, 3649.
45. H. Sirringhaus, T. Kawase, R.H. Friend, T. Shimoda, M. Inbasekaran, W. Wu and E.P. Woo, *Science*, 2000, **290**, 2123.
46. Polymer Science: A Comprehensive Reference 2012, Pages 147–175 Volume 8: Polymers for Advanced Functional Materials Ink-Jet Printing of Functional Polymers for Advanced Applications J. Perelaer, U.S. Schubert
47. P.J. Smith and A. Morrin, *J. Mat. Chem.*, 2012, **22**, 10965.
48. A. Abulikemu, E.H. Da-as, H. Haverinen, D. Cha, M.A. Malik and G.E. Jabbour, *Angew. Chem*, 2014, **126**, 430.
49. P. Krober, J. T. Delaney, J. Perelaer and U.S. Schubert, *J. Mater. Chem.*, 2009, **19**, 5234.
50. P. Calvert, *Chem. Mater.*, 2001, **13**, 3299.
51. A.G. MacDiarmid, *Angew. Chem. Int. Ed.*, 2001, **40**, 2581.
52. I. McCulloch, M. Heeney, C. Bailey, K. Genevicius, I. MacDonald, M. Shkunov, D. Sparrowe, S. Tierney, R. Wagner, W. Zhang, M.L. Chabinye, R.J. Kline, M.D. McGehee and M.F. Toney, *Nat. Mater.*, 2006, **5**, 328.
53. F. Garnier, R. Hajlaoui, A. Yassar, P. Srivastava, *Science*, 1994, **265**, 1864.
54. S. Sivaramakrishnan, P.J. Chia, Y.C. Yeo, L.L.Chua and P.K.H. Ho, *Nat. Mater.*, 2007, **6**, 149.
55. S. Kirchmeyer and K. Reuter, *J. Mat. Chem.*, 2005, **15**, 2077.
56. A. De La Fuente Vornbrock, D. Sung, H. Kang, R. Kitsomboonloha and V. Subramanian, *Org. Electron.*, 2010, **11**, 2037.
57. A.C. Arias, S.E. Ready, R. Lujan, W.S. Wong, K.E. Paul, A. Salleo, M.L. Chabinye, R. Apte, A.S. Robert, Y. Wu, P. Lium and B. Ong, *Appl. Phys. Lett.*, 2004, **85**, 3304.
58. Q. Liu, Z. Liu, X. Zhang, L. Yang, N. Zhang, G. Pan, S. Yin, Y. Chen and J. Wei, *Adv. Funct. Mater.*, 2009, **19**, 894.
59. J. Bharathan and Y. Yang, *Appl. Phys. Lett.*, 1998, **72**, 2660.
60. L. Groenendaal, F. Jonas, D. Freitag, H. Pielartzik, R. Reynolds, *Adv. Mater.*, 2000, **12**, 481.
61. Y.H. Kim, C. Sachse, M.L. Machala, C. May, L. Müller-Meskamp and K. Leo, *Adv. Funct. Mater.*, 2011, **21**, 1076.
62. Y.J. Xia, K. Sun and J.Y. Ouyang, *Adv. Mater.*, 2012, **24**, 2436.
63. R.M. Meixner, D. Cibis, K. Krueger and H. Goebel, *Microsyst. Technol.*, 2008, **14**, 1137.
64. D. Cibis and K. Krueger, 1st international conference on ceramic interconnect and ceramic microsystems technologies, Baltimore, 2005.
65. B. Derby and N. Reis, *MRS Bull*, 2003, **28**, 816.
66. J.E. Anthony, A. Facchetti, M. Heeney, S.R. Marder and X. Zhan, *Adv. Mater.*, 2010, **22**, 3876.

67. K.J. Baeg, D. Khim, D.Y. Kim, S.W. Jung, J.B. Koo, I.K. You, H. Yan, A. Facchetti and Y.Y. Noh, *J. Polym. Sci. B Polym. Phys.*, 2011, **49**, 62.
68. S. Magdassi, M. Grouchko, O. Berezin and A. Kamyshny, *ACS Nano*, 2010, **4**, 1943.
69. J. Perelaer, B.J. Gans, U.S. Schubert, *Adv. Mater.*, 2006, **18**, 2101.
70. T.H.J. Van Osch, J. Perelaer, A.W.M. Laat and U.S. Schubert, *Adv. Mater.*, 2008, **20**, 343.
71. K. Ghaffarzadeh and H. Zervos, *Silver & Copper Inks & Pastes and Beyond*, Conductive Ink Markets 2012-2018, IDTechEx, Cambridge, 2012.
72. Y. Chang, D.Y. Wang, Y.L. Tai and Z.G. Yang, *J. Mater. Chem.*, 2011, **22**, 25296.
73. S.B. Fuller, E.J. Wilhelm and J.M. Jacobson, *J. Microelectromech. Syst.*, 2002, **11**, 54.
74. D. Kim, S. Jeong, B.K. Park and J. Moon, *Appl. Phys. Lett.*, 2006, **89**, 264101.
75. J. Doggart, Y. Wu, P. Liu and S. Zhu, *ACS Appl. Mater. Interfaces*, 2010, **2**, 2189.
76. D. Kim and J. Moon, *Electrochem. Solid-State Lett.*, 2005, **8**, J30.
77. L. Polavarapu, K.K. Manga, H.D. Cao, K.P. Loh and Q.H. Xu, *Chem. Mater.*, 2011, **23**, 3273.
78. L. Polavarapu, K.K. Manga, K. Yu, P.K. Ang, H.D. Cao, J. Balapanuru, K.P. Loh and Q.H. Xu, *Nanoscale*, 2011, **3**, 2268.
79. R. Shankar, L. Groven, A. Amert, K.W. Whites and J.J. Kellar, *J. Mater. Chem.*, 2011, **21**, 10871.
80. S.K. Volkman, Y. Pei, D. Redinger, S. Yin, and V. Subramanian, *Mater. Res. Soc. Symp. Proc.*, 2004, **814**, 17.8.1.
81. K.J. Lee, B.H. Jun, T.H. Kim and J. Joung, *Nanotechnology*, 2006, **17**, 2424.
82. S. Magdassi, M. Grouchko, D. Toker, A. Kamyshny, I. Balberg and O. Millo, *Langmuir*, 2005, **21**, 10264.
83. A. Kamyshny, J. Steinke and S. Magdassi, *The Open Appl. Phys. Journal*, 2011, **4**, 19.
84. *Inkjet!: History, Technology, Markets, and Applications*, ed. F.J. Romano, Digital Printing Council PIA/GATF Press, Pittsburgh, 2008, pp.328.
85. A.L. Dearden, P.J. Smith, D.-Y. Shin, N. Reis, B. Derby and P. O'Brien, *Macromol. Rapid. Commun.*, 2005, **26**, 315.
86. W.R. Vest, in *Ceramic Films and Coatings*, ed. J.D. Wachtman and R.A. Haber, Noyes Publications, Park Ridge, 1993, pp 303-347.
87. K.F. Teng and R.W. Vest, *IEEE Electron. Device Lett.*, 1988, **9**, 591.
88. S.F. Jahn, T. Blaudeck, R.R. Baumann, A. Jakob, P. Ecorchard, T. Ruffer, H. Lang and P. Schmidt, *Chem. Mater.*, 2010, **22**, 3067.
89. C.B. Walker and J. A. Lewis, *J. Am. Chem. Soc.*, 2012, **134**, 1419.
90. J. Perelaer, P.J. Smith, D. Mager, D. Soltman, S.K. Volkman, V. Subramanian, J.G. Korvink and U.S. Schubert, *J. Mater. Chem.*, 2010, **20**, 8446.
91. J.R. Greer and R.A. Street, *Acta Mater.*, 2007, **55**, 6345.
92. J. J. P. Valetton, K. Hermans, C. W. M. Bastiaansen, D. J. Broer, J. Perelaer, U. S. Schubert, G. P. Crawford and P.J. Smith, *J. Mat. Chem.*, 2010, **20**, 543.
93. M. Hosel and F.C. Krebs, *J. Mater. Chem.*, 2012, **22**, 15683.
94. M. Grouchko, A. Kamyshny, C.F. Mihailescu, D.F. Anghel and S. Magdassi, *ACS Nano*, 2011, **5**, 3354.
95. H. Meier, U. Löffelmann, D. Mager, P.J. Smith and J.G. Korvink, *Phys. Status Solidi A*, 2009, **206**, 1626.
96. J.-T. Wu, S.L.-C. Hsu, M.-H. Tsai, Y.-F. Liu and W.-S. Hwang, *J. Mater. Chem.*, 2012, **22**, 15599.
97. D.L. Shulz, C.J. Curtis and D.S. Ginley, *Solid-State Lett.*, 2001, **4**, C58.
98. M. Grouchko, A. Kamyshny and S. Magdassi, *J. Mater. Chem.*, 2009, **19**, 3057.
99. D. Li, D. Sutton, A. Burgess, D. Graham and P.D. Calvert, *J. Mater. Chem.*, 2009, **19**, 3719.
100. S. Jeong, K. Woo, D. Kim, S. Lim, J.S. Kim, H. Shin, Y. Xia and J. Moon, *Adv. Funct. Mater.*, 2008, **18**, 679.
101. Michael Grouchko, Alexander Kamyshny and Shlomo Magdassi, *J. Mater. Chem.*, 2009, **19**, 3057-3062 | 3057
102. Y.I. Lee and Y.H. Cho, *J. Mater. Chem.*, 2012, **22**, 12517.
103. J. Wang and M. Musameh, *Analyst*, 2004, **129**, 1.
104. L. Zhang, C. Di, G. Yu and Y. Liu, *J. Mater. Chem.*, 2010, **20**, 7059.
105. X. Zhou, J.Y. Park, S.M. Huang, J. Liu and P.L. McEuen, *Phys. Rev. Lett.*, 2005, **95**, 146805.
106. R.S. Ruoff, J. Tersoff, D.C. Lorents, S. Subramoney and B. Chan, *Nature*, 1993, **364**, 514.
107. T.J. Simmons, D. Hashim, R. Vajtai and P.M. Ajayan, *J. Am. Chem. Soc.*, 2007, **129**, 10088.
108. D.S. Hecht, L. Hu and G. Irvin, *Adv. Mater.*, 2011, **23**, 1482.
109. K. Kordás, T. Mustonen, G. Tóth, H. Jantunen, M. Lajunen, C. Soldano, S. Talapatra, S. Kar, R. Vajtai and P.M. Ajayan, *Small*, 2006, **2**, 1021.
110. N. Nakashima, *Int. J. Nanosci.*, 2005, **4**, 119.
111. T.J. Simmons, D. Hashim, R. Vajtai and P.M. Ajayan, *J. Am. Chem. Soc.*, 2007, **129**, 10088.
112. M.J. O'Connell, S.M. Bachilo, C.B. Huffman, V.C. Moore, M.S. Strano, E.H. Haroz, K.L. Rialon, P.J. Boul, W.H. Noon, C. Kittrell, J. Ma, R.H. Hauge, R.B. Weisman and R.E. Smalley, *Science*, 2002, **297**, 593.
113. M.F. Mabrook, C. Pearson, A.S. Jombert, D.A. Zeze and M.C. Petty, *Carbon*, 2009, **47**, 752.
114. P. Beecher, P. Servati, A. Rozhin, A. Colli, V. Scardaci, S. Pisana, T. Hasan, A.J. Flewitt, J. Robertson, G.W. Hsieh, F.M. Li, A. Nathan, A.C. Ferrari and W.I. Milne, *J. Appl. Phys.*, 2007, **102**, 043710.
115. D.H. Kim, H.J. Shin, H.S. Lee, J. Lee, B.L. Lee, W.H. Lee, J.H. Lee, K. Cho, W.J. Kim, S.Y. Lee, J.Y. Choi and J.M. Kim, *ACS Nano*, 2012, **6**, 662.
116. N. Rouhi, D. Jain and K. Zand, *Adv. Mater.*, 2011, **23**, 94.
117. S. Park and R.S. Ruoff, *Nat. Nanotechnol.*, 2009, **4**, 217.
118. D.V. Kosynkin, A.L. Higginbotham, A. Sinitskii, J.R. Lomeda, A. Dimiev, B.K. Price and J.M. Tour, *Nature*, 2009, **458**, 872.
119. D. Li, *Science*, 2008, **320**, 1170.
120. L. Jiao, L. Zhang, X. Wang, G. Diankov and H. Dai, *Nature*, 2009, **458**, 877.
121. X. Li, W. Cai, J. An, S. Kim, J. Nah, D. Yang, R. Piner, A. Velamakanni, I. Jung, E. Tutuc, S.K. Banerjee, L. Colombo and R.S. Ruoff, *Science*, 2009, **324**, 1312.
122. D. Wei and Y. Liu, *Adv. Mater.*, 2010, **22**, 3225.
123. C.D. Zangmeister, *Chem. Mater.*, 2010, **22**, 5625.
124. S. Stankovich, D.A. Dikin, R.D. Piner, K.A. Kohlhaas, A. Kleinhammes, Y. Jia, Y. Wu, S.T. Nguyen and R.S. Ruoff, *Carbon*, 2007, **45**, 1558.
125. L.J. Cote, R. Cruz-Silva and J. Huang, *J. Am. Chem. Soc.*, 2009, **131**, 11027.

126. *US Pat.*, 20120170171 A1, 2012.
127. L. Huang, Y. Huang, J. Liang, X. Wan, Y. Chen, *Nano Res.*, 2011, **4**, 675.
128. F. Torrisi, T. Hasan, W. Wu, Z. Sun, A. Lombardo, T.S. Kulmala, G.W. Hsieh, S. Jung, F. Bonaccorso, P.J. Paul, D. Chu and A.C. Ferrari, *ACS Nano*, 2012, **6**, 2992.
129. D. Kong, L.T. Le, Y. Li, J.L. Zunino and W. Lee, *Langmuir*, 2012, **28**, 13467.
130. L.V. Gregor, *IBM J. Res. Dev.*, 1968, **12**, 140.
131. J.C. Anderson, *J. Vac. Sci. Technol.*, 1972, **9**, 1.
132. C.J. Drury, C.M. Musaers, C.M. Hart, M. Matters, D.M. de Leeuw, *Appl. Phys. Lett.*, 1998, **73**, 108.
133. Z. Bao, V. Kuck, J.A. Rogers and M. Paczkowski, *Adv. Funct. Mater.*, 2002, **12**, 526.
134. L.L. Chua, P.K.H. Ho, H. Sirringhaus and R.H. Friend, *Appl. Phys. Lett.*, 2004, **84**, 3400.
135. A. Facchetti, *Nat. Mater.*, 2008, **7**, 839.
136. M.P. Walsler, W.L. Kalb, T. Mathis and B. Batlogg, *Appl. Phys. Lett.*, 2009, **95**, 233301.
137. B.N. Pal, B.M. Dhar, K.C. See and H.E. Katz, *Nat. Mater.*, 2009, **8**, 898.
138. M.M. Ling MM, Z. Bao, *Chem. Mater.*, 2004, **16**, 4824.
139. D. Redinger, S. Molesa, S. Yin, R. Farschi and V. Subramanian, *IEEE Trans. Electron. Devices*, 2004, **51**, 1978.
140. Y. Chen, Y. Xu, K. Zhao, X. Wan, J. Deng and W. Yan, *Nano Res.*, 2010, **3**, 714.
141. S. Jeong, S. Lee, D. Kim, H. Shin and J. Moon, *J. Phys. Chem. C*, 2007, **111**, 16083.
142. S. Fabiano, C. Musumeci, Z. Chen, A. Scandurra, H. Wang, Y.L. Loo, A. Facchetti and B. Pignataro, *Adv. Mater.*, 2012, **24**, 951.
143. T.B. Singh, F. Meghdadi, S. Günes, N. Marjanovic, G. Horowitz, P. Lang, S. Bauer and N.S. Sariciftci, *Adv. Mater.*, 2005, **17**, 2315.
144. Y. Liu, K. Varshney and T. Cui, *Macromol. Rapid Commun.*, 2005, **26**, 1955.
145. A. Facchetti, M.H. Yoon and T.J. Marks, *Adv. Mater.*, 2005, **17**, 1705.
146. T.B. Singh, S. Günes, N. Marjanović, N.S. Sariciftci and R. Menon, *J. Appl. Phys.*, 2005, **97**, 114508.
147. S.Y. Yang, S.H. Kim, K. Shin, H. Jeon, C.E. Park, *Appl. Phys. Lett.*, 2006, **88**, 173507.
148. Y. Jang, D.H. Kim, Y.D. Park, J.H. Cho, M. Hwang and K. Cho, *Appl. Phys. Lett.*, 2006, **88**, 072101.
149. M.E. Roberts, N. Queraltó, S.C.B. Mannsfeld, B.N. Reinecke, W. Knoll and Z. Bao, *Chem. Mater.*, 2009, **21**, 2292.
150. C. Kim, Z.M. Wang, H.J. Choi, Y.G. Ha, A. Facchetti and T.J. Marks, *J. Am. Chem. Soc.*, 2008, **130**, 6867.
151. M.H. Yoon, H. Yan, A. Facchetti and T.J. Marks, *J. Am. Chem. Soc.*, 2005, **127**, 1038810395.
152. H. Kang, D. Soltman and V. Subramanian, *Langmuir*, 2010, **26**, 11568.
153. D. Soltman, B. Smith, H. Kang, S.J. Morris and V. Subramanian, *Langmuir*, 2010, **26**, 15686.
154. S. Chung, J. Jang, J. Cho, C. Lee, S.K. Kwon and Y. Hong, *Jpn. J. Appl. Phys.*, 2011, **50**, 03CB05.
155. S. Jeong, D. Kim and J. Moon, *J. Phys. Chem. C*, 2008, **112**, 5245.
156. S.H. Ko, H. Pan, C.P. Grigoropoulos, C.K. Luscombe, J.M.J. Fréchet and D. Poulikakos, *Appl. Phys. Lett.*, 2007, **90**, 141103.
157. M. Halik, H. Klauk, U. Zschieschang, T. Kriem, G. Schmid, W. Radlik and K. Wussow, *Appl. Phys. Lett.*, 2002, **81**, 289.
158. J.H. Cho, J. Lee, Y. Xia, B. Kim, Y. He, M.J. Renn, T.P. Lodge and C.D. Frisbie, *Nat. Mater.*, 2008, **7**, 900.
159. G. Eda, G. Fanchini and M. Chhowalla, *Nat. Nanotechnol.*, 2008, **3**, 270.
160. D.A. Dikin, S. Stankovich, E.J. Zimney, R.D. Piner, G.H.B. Dommett, G. Evmenenko, S.B.T. Nguyen and R.S. Ruoff, *Nature*, 2007, **448**, 457.
161. H.Y. Jeong, J.Y. Kim, J.W. Kim, J.O. Hwang, J.E. Kim, J.Y. Lee, T.H. Yoon, B.J. Cho, S.O. Kim, R.S. Ruoff and S.Y. Choi, *Nano Lett.*, 2010, **10**, 4381.
162. S.K. Lee, H.Y. Jang, S. Jang, E. Choi, B.H. Hong, J. Lee, S. Park and J.H. Ahn, *Nano Lett.*, 2012, **12**, 3472.
163. J.T. Delaney, P.J. Smith and U.S. Schubert, *Soft Matter*, 2009, **5**, 4866.
164. B.J. Derby, *Mater. Chem.*, 2008, **18**, 5717.
165. T. Boland, T. Xu, B. Damon, X. Cui, *Biotechnol. J.*, 2006, **1**, 910.
166. F. Rusmini, Z.Y. Zhong and J. Feijen, *Biomacromolecules*, 2007, **8**, 1775.
167. G. Arrabito and B. Pignataro, *Anal. Chem.*, 2012, **84**, 5450.
168. S. Di Risio and N. Yan, *Macromol. Rapid Commun.*, 2007, **28**, 1934.
169. J. Sumerel, J. Lewis, A. Doraiswamy, L.F. Deravi, S.L. Sewell, A.E. Gerton, D.W. Wright and R.J. Narayan, *Biotechnol. J.*, 2006, **1**, 976.
170. L. Setti, A. Fraleoni-Morgera, B. Ballarin, A. Filippini, D. Frascaro and C. Piana, *Biosens. Bioelectron.*, 2005, **20**, 2019.
171. M. Graber and D. Combes, *Enzyme Microb. Tech.*, 1989, **11**, 673.
172. G. Arrabito, C. Musumeci, V. Aiello, S. Libertino, G. Compagnini and B. Pignataro, *Langmuir*, 2009, **25**, 6312.
173. G. Arrabito and B. Pignataro, *Anal. Chem. (Lett.)*, 2010, **82**, 3104.
174. G. Arrabito, C. Galati, S. Castellano and B. Pignataro, *Lab Chip*, 2013, **13**, 68.
175. C.J. Ferris, K.J. Gilmore, S. Beirne, D. McCallum, G.G. Wallace and M. Panhuis, *Biomater. Sci.*, 2013, **1**, 224.



Advances in upscalable wet methods and ink formulations are improving the properties of printed molecular thin films along with the performance of printed electronic devices.